ICE CHARACTERISTICS IN THE SEASONAL SEA ICE ZONE

Peter Wadhams

Scott Polar Research Institute, Cambridge CB2 1ER, England

INTRODUCTION

The seasonal sea ice zone has been defined as the area between the minimum and maximum seasonal ice limits plus the region of the ice margin that is significantly affected by the ice-ocean boundary. This definition includes almost all of the Antarctic ice cover, the ice in the marginal seas around the Arctic and the ice cover overlying the shelves of the Arctic Ocean itself. Such a vast area includes a very large number of ice types. To simplify our review, we shall therefore consider four reasonably well-defined ice regimes. These are:

Landfast ice. This is ice which grows seaward from a coast and which stays in place throughout the winter, breaking up and drifting away, or melting, in spring. Off a gently sloping shore facing an unbounded sea, such as the Beaufort Sea coasts of Alaska and Canada, the landfast ice is stabilized by the presence of grounded pressure ridges in its outermost parts, and therefore extends out to the draft limit of such ridges, about 20 m water depth. In constricted channels, such as the Canadian Arctic Archipelago, the landfast ice fills the whole width of the channel, regardless of water depth which may be 200 m or more, and should really be described as "quasi-fast ice" since the stabilization is not complete, allowing some movement and deformation throughout the winter.

The shear zone is formed when the permanent polar pack moves against a fixed boundary of either land or landfast ice. The shearing and convergence of the pack's motion generates a band of highly deformed ice which has a higher density of ridging than the ice further out in the ocean. The most highly developed shear zone extends from the north coast of Alaska across the fringe of the Canadian Arctic Archipelago to northeast Greenland. Because the shear zone generally overlies shelf areas bearing mineral resources, a knowledge of its properties is of great practical importance; also, it represents the boundary condition for models of Arctic Ocean ice drift.

The marginal ice zone (MIZ) is that part of the ice cover which is close enough to the open ocean boundary to be affected by its presence. Therefore, all cold drift currents (e.g., East Greenland, Labrador) can be considered as MIZ, as well as any ice lying within 150-200 km of an open ocean ice edge. Ice in the MIZ has much greater freedom of movement than ice in the central polar pack, and a number of phenomena of ice-ocean-atmosphere interaction occur which are peculiar to this area. The best developed MIZ's lie along the northern edge of the Antarctic ice cover and around the North Atlantic fringes of the Arctic, since in both these regions the ice abuts a wide ocean basin, but MIZ conditions are also found in the Bering Sea and Baffin Bay in winter.

The Antarctic ice cover is considered separately because almost all of the Antarctic is a seasonal ice zone, the ice cover shrinking in summer to less than 25% of its winter maximum. Phenomena peculiar to the MIZ are considered under that heading, but the whole Antarctic ice cover has considerable freedom since it is a divergent cover which is constantly advecting northward.

In addition, there are areas of the Arctic possessing a seasonal dynamic ice cover which are not MIZ's because of their remoteness from the open ocean. These regions include the interior of Baffin Bay and parts of the Bering Sea and Sea of Okhotsk. We shall not consider these areas as a separate category, since the geometrical and dynamical properties of the ice cover are intermediate between the MIZ and the permanent polar ice.

In the review which follows we shall concentrate on unsolved problems rather than on known facts, and we shall have frequent recourse to speculation.

FAST ICE

Occurrence and Development

True shorefast ice, that is ice which is fast both to the shore and to anchoring points on the seabed, occurs in winter around the entire rim of the Arctic Ocean as well as in many sub-Arctic areas and around the coasts of Antarctica. Even on the steepest shoreline, or in places where rapid currents or large tides prevent normal fast ice formation, there is usually an icefoot which is wide enough to facilitate sledge travel in winter. The most extensive development of fast ice occurs where the coast shelves vary gently, i.e., in the Mackenzie Delta area of Canada and in the Laptev Sea and other shelf areas of northern Siberia. Ice forms early in the winter along coasts because of:

(i) the shallow water which reduces the depth of convection necessary to cool the water column to the freezing point;

(ii) the lower salinity caused by river discharge;

(iii) the generally more quiescent sea surface conditions.

"(i)" is the major factor. The genesis of a consolidated ice sheet is fairly well known. In rough water the early stages include frazil, grease, and pancake ice, and since these exist throughout the winter in the marginal ice zone they are dealt with under the MIZ in the section on young ice forms. In smooth water the frazil stage passes relatively quickly via nilas into a consolidated sheet, from which brine drains as it grows thicker (Cox and Weeks, 1974).

The subsequent development of the fast ice zone has been reviewed by Kovacs and Mellor (1974) for the case of the Beaufort Sea. It depends on the shape of the shoreline, the bathymetry and the motion of the offshore pack, and three typical stages are shown in Figure 1 (after Kovacs and Mellor). Beyond the icefoot and the tidal crack(s) the fast ice grows seaward until it encounters the moving polar pack. The events which happen at this stage largely determine the winter morphology of the fast ice zone. In the Beaufort Sea the pack ice tends to be driven towards land by the wind field. Each shoreward drive of the pack deforms the nascent fast ice sheet. If the drive is of short duration and limited intensity, only the outer part of the ice sheet will be affected, yielding an irregular and low-lying relief of rafted blocks. If the pressure is higher and more prolonged, the ice sheet will be deformed into ridges which may grow large enough to become grounded. The grounded ridge then provides an anchoring point for the fast ice sheet. Other grounded ridges originate from the pack itself but become incorporated in the fast ice zone, as do grounded ice island fragments, driven ashore during autumn storms. More extensive and prolonged pressure may cause further deformation into a continuous field of rubble-like hummocks or oriented pressure ridges. Such a hummock field may remain in the fast ice zone or may break away and drift with the pack. Eventually, the fast ice sheet becomes thick enough and strong enough to resist further deformation and takes on its permanent winter morphology. The distribution of grounded ridges is important because of their bottom scouring effect. The typical winter form of the fast ice is seen clearly in Figure 2 (taken from Wadhams (1976), which is a SLAR image obtained in April off the Tuktoyaktuk Peninsula. The inner fast ice zone consists of a smooth sheet. As the distance from land increases scattered floes or ridges begin to appear, embedded in the otherwise smooth ice, while there is a final outer zone of heavily ridged ice before a flaw lead separates the fast ice from the shear zone of the moving pack.

The outer limit of the fast ice zone is roughly the draft limit of grounded pressure ridges, and off Alaska occurs at a water depth of about 18 m (Stringer, 1974), but with occasional bulges, possibly temporary, out to 27 m. It is possible that parts of the shear zone may become temporarily attached to the fast ice zone, especially if the occasional ridge in the zone is deep enough to touch bottom, but not enough is known about shear zone dynamics for us to know the extent of this "stick-slip" phenomenon.

Although rigidly bound to anchoring points, the fast ice has been observed to make small movements during the winter. Cooper (1974) measured displacements of the order of 10 m in Mackenzie Bay. Tucker et al. (1979a) observed ice motion with a laser ranging system from Narwhal and Cross Islands off the Alaskan coast. In 1976 they observed similar small displacements, but in 1977 the displacements in the outer fast ice zone were much greater - up to 160 m. They ascribed the small progressive displacements to thermal expansion of the ice, and the larger motions (which were poorly correlated with the local wind) to the compressive effect of the offshore pack moving against the fast ice. The ice always returned to approximately its former position after a large excursion of this kind. The cause and magnitude of these motions are important because of the possible danger to drilling rigs operating through artificially

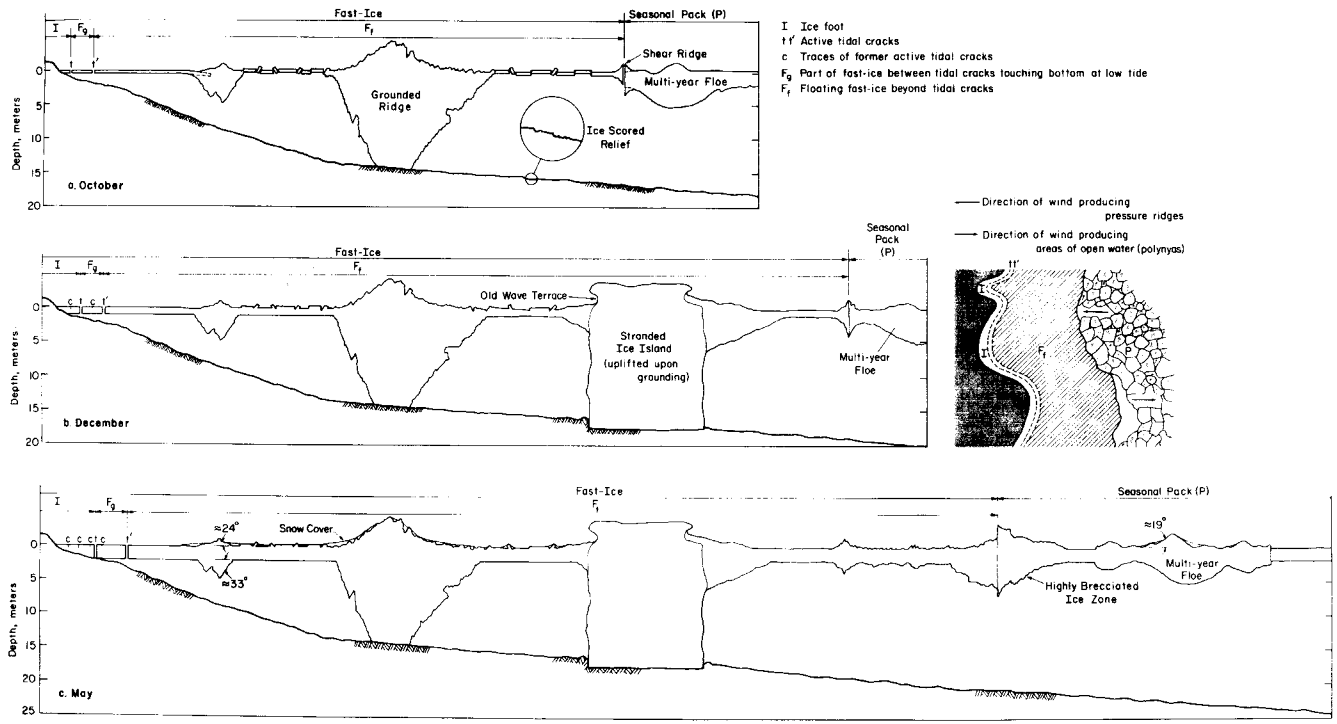

Figure 1. Three stages in the development of the fast ice zone (after Kovacs and Mellor, 1974)

thickened fast ice sheets. A further possible cause of fast ice motion is winter storm surges; by temporarily raising sea level, they facilitate ice push onto beaches.

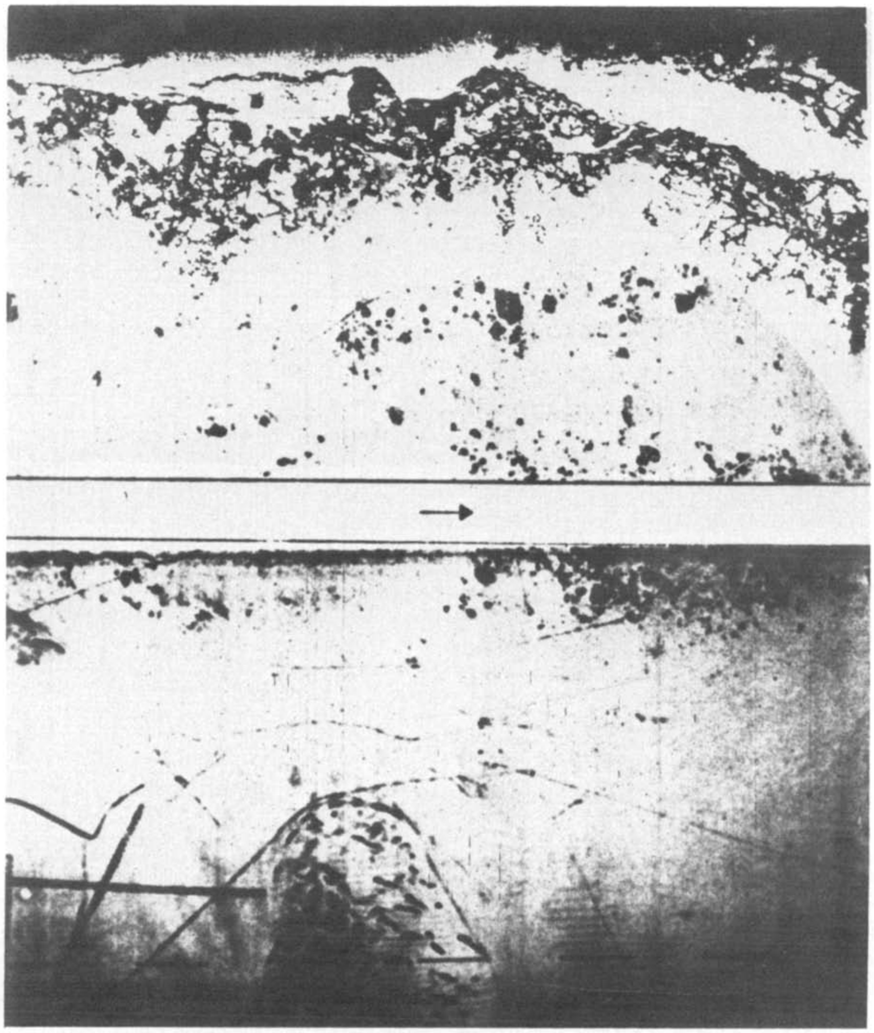

Figure 2. SLAR Imagery of Beaufort Sea fast ice, 26 April 1975.

Fast Ice in Constricted Channels

So far we have considered ice which is fast both to the shore and to the seabed. Another type of fast ice is fast only to the shore and is held in place as a consolidated sheet by the restrictive geometry of the channels and bays in which it grows. Such ice fills the channels of the Canadian Arctic Archipelago and the channels between the Soviet Arctic islands.

A review of ice in the Canadian Arctic has been given by Lindsay (1969), who described the characteristics of ice in the Queen Elizabeth Islands (i.e., the islands north of Parry Channel). On average the new ice forms a consolidated sheet by 15 October, and by the end of May has reached a thickness of 2.0 m. It breaks up by about 15 July, after which the broken ice either partially melts and partially drifts out of the channels in a generally northwest-to-southwest direction under the prevailing wind and current, or else stays around to choke the channels until the next ice season begins. Thus, ice years can be divided into "good", "average" or "bad" from the point of view of navigation, depending on the behavior of the ice after breakup. 1962 was a good year and 1964 a bad, and the difference is shown in the percentage of sea area among the channels that remained ice-covered:

1962	June	87	July	48	August	32	September	65
1964		90		85		72		79

It is seldom that two good years occur in succession, since the removal of the winter ice in the first good summer permits Polar ice to enter the western channels, mainly via Gustav Adolf Sea and M'Clure Strait, and to move further east in the following summer to disrupt navigation in Parry Channel. Thus, there is a natural period of 2-4 years in ice conditions, on which are superimposed fluctuations due to climate and wind variations. Lindsay analyzed the natural history of good and bad years in various parts of the Queen Elizabeth Islands in a quest for an "indicator area" whose behavior in autumn could give a prediction of the ice conditions to be expected in the following summer. He suggested Jones Sound as such an indicator, since the patterns of freeze-up and break-up occur in a number of distinct stages whose dates correlate well with the "goodness" or "badness" of the ice year.

Even after the ice sheet becomes consolidated its freedom of movement is greater than that of shorefast ice. Wetzel et al. (1974) set up an acoustic transponder system in November on the ice of the Belcher Channel south of Cornwall Island, using a bottom reference. They found that instead of the 10 m motions in the Beaufort Sea, the ice moved 100 m in the first seven days and finally drifted bodily out of range of the transponder at a rate of 300 m in 12 minutes. While within range the ice moved in elliptical orbits at the inertial frequency, but with net translations of at least 100 m per orbit. It is probable that a very wide sheet such as this is able to suffer internal deformation, say along a line of weakness near the shore, driven by wind or current stress integrated over a large area.

Truly free ice movement in the Arctic Archipelago occurs only after break-up and before the consolidation of the new season's ice, i.e., between June and September. The average movement is eastward, in accord with the mean water flow, but there are many exceptions. There appears to be a gyre within Parry Channel, with a westward flow along the north side and eastward along the south. Two ice islands have been tracked through these channels. The first, T-1 in 1959, followed the route Gustav Adolf Sea - Byam Martin Channel -Viscount Melville Sound - McClintock Channel. The second, Station Charlie, entered M'Clure Strait in 1964 after a complete circuit of the Beaufort Gyre in the Arctic Ocean and is thought to have broken up in Lancaster Sound. Thus, there is a considerable flux of polar ice from the Arctic Ocean into the channels of the Arctic Archipelago. Verrall et al. (1974), however, found when measuring the summer drift by tracking buoys placed on ice that there was a westward drift through M'Clure Strait during the time of the experiment and no definite translation in Viscount Melville Sound. The direction of drift was, in fact, in accord with Zubov's rule (Zubov, 1945) for freely drifting floes, which states that the motion is parallel to the isobars (i.e., to the geostrophic wind) and is of magnitude about 1% of the geostrophic wind W, which is given by

$$W = \frac{1}{2\omega\rho \sin \phi} |\nabla P| \tag{1}$$

where ω is the angular velocity of the Earth, ρ is air density, ϕ is latitude and ∇P is the horizontal atmospheric pressure gradient. Zubov implies that the turning of the ice relative to the surface wind is equal and opposite to the turning of the surface wind relative to the geostrophic wind. It seems that summer ice drift, where internal stresses are negligible, can best be predicted from this rule in direction, although perhaps not in magnitude. Some important questions regarding ice in constricted channels are:

(i) What is the contribution of Arctic Ocean ice to the mass balance of the Arctic Archipelago?

(ii) Do we now have indicators which will predict the goodness or badness of the navigation season from the dates of freeze-up, the ice characteristics at freeze-up or from meteorological indicators?

(iii) Is there a critical size of basin or channel above which fast ice never consolidates during the winter? In other words, are size and shape the major factors determining whether or not a basin grows a fast ice cover, or are the mean wind and current fields equally important? It is noteworthy that basins do not have to be completely closed to possess a fast ice cover; Lancaster Sound, for instance, is open to the east.

(iv) Can we locate all of the bays and channels where geometry permits fast ice to remain throughout the summer, so that it grows for many years and acquires a very great thickness (12 m or more) before it finally breaks out? Observations of such ice are discussed in Walker and Wadhams (1979), and such areas may be especially suitable for studies of the basic physics of sea ice.

Wave Propagation Through Fast Ice

Fast ice offers the closest approach in nature to an ideal uniform floating ice sheet. In such an ice sheet it is possible for a variety of wave modes to propagate (Anderson, 1963). We shall consider the one type which possesses geophysical importance, the flexural-gravity wave.

This is a normal surface gravity wave which is coupled to the ice and propagates partly as a wave in the water with normal elliptical particle orbits, and partly as a sinusoidal wave in the ice sheet. Such waves can be generated in two ways, only one of which is well understood. The known way is by an ocean swell at an ice-water boundary passing into the ice and propagating through it; the change in propagation characteristics will cause a portion of the incident energy to be reflected at the boundary. The unknown way is by wind blowing over the ice; the mechanism of wind-ice coupling is not known but is presumably similar to the mechanism of wave generation by a moving load (e.g., vehicles moving on ice or aircraft landing on sea ice runways).

If the ice is assumed to be perfectly elastic, the dispersion relation of such a wave is given by

$$L\,k^5 + (\rho_w g - \rho_i h\,\omega^2)\,k - \rho_w\,\omega^2 = 0 \tag{2}$$

where $k = 2\pi/\lambda$, with λ the wavelength in the ice; $L = E\,h^3/12(1-\nu^2)$ is the flexural rigidity; E is Young's modulus; ρ_i,ρ_w are ice and water densities; h is ice thickness; ν is Poisson's ratio and ω is the angular frequency. This was known, almost correctly, as far back as 1887 (Greenhill). As well as a real solution for k, i.e., the propagating wave, there are two complex solutions which produce local waves close to the ice-water boundary. These waves disappear within one or two wavelengths of the boundary, but may be important in causing ice breakup (see section on Mechanisms of breakup). The phase and group velocities of the propagating wave are shown in Figure 3; at long periods the propagation is similar to that of a swell on the open sea, while at very short periods it resembles a wave on an elastic sheet. Flexural-gravity waves have been measured in the central Arctic pack by gravimeters (Hunkins, 1962) and on fast ice by wire strainmeters (Goodman et al., 1975) which record the surface strain due to the flexure.

Flexural-gravity waves can decay by many mechanisms, e.g., by encountering ridges, changes in ice thickness or properties, or leads. In the absence of such imperfections in the ice sheet the major mechanism of decay is the lossy nature of the sea ice itself. This has been modelled in two ways. One was to apply a creep-type flow law to the ice and to consider pure elasticity as the determinant of propagation characteristics while the creep determines the energy loss (Wadhams, 1973a). A later, and more rigorous approach has been to use a temperature-dependent visco-elastic constitutive law for the ice and derive the propagation characteristics afresh (Squire and Allan, 1979; Squire, 1979), when a decaying propagating wave is obtained.

Mechanisms of Breakup

The dates of ice breakup in the shorefast ice and in channel ice are usually predictable to

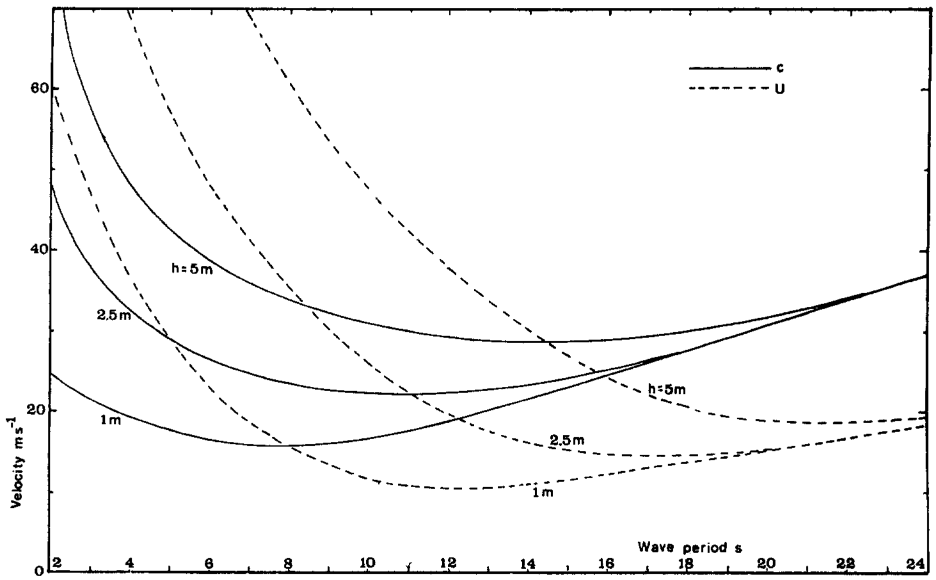

Figure 3. Phase (C) and group (U) velocities of flexural-gravity waves in ice of different thicknesses.

within a few days (Bilello, 1979) and the sequence of breakup by area is also to some extent predictable. However, detailed mechanisms are not known, except that breakup usually occurs at a time of strong wind and after a period of weakening of the ice cover by superficial solar melting or by bottom melting due to an influx of fresh water under the ice from newly swelling rivers. Some possible mechanisms include:

(i) Breakup by propagating waves. The flexural-gravity waves described in the preceding section propagate through a uniform ice sheet with a constant or decreasing amplitude, and therefore will not cause fracture at a distance inside the ice sheet. However, no ice sheet is completely uniform, and all sheets are subject to thickness variations and to strength variations due to the presence of thermal tension cracks (Milne, 1972) or other cracks which weaken its structure and which, at the crack tip, multiply the local stress. Sea ice therefore displays a variable fracture toughness which is much lower than that of pure laboratory ice (Goodman and Tabor, 1978). Thus a wave may cause breakup when it enters such an area of relative weakness. The plate equations describing the deformation due to such a wave are given by Assur (1963).

Other possibilities depend on the dynamical behavior of waves entering shoaling water. In the case of shorefast ice, as the wave approaches the shore it steepens (the dispersion relation given in (2) is for deep water, and in shallow water the velocity for a given frequency is reduced, Wadhams, 1973b) and therefore the bending stress on the overlying ice sheet is increased. Further, the mean sea level is subject to a "set down" followed by a "set up" (Le-

Blond and Mysak, 1978) which also cause curvature of the sea surface. Thirdly, there is the possibility of wave reflection from the coast or from irregularities such as grounded ice islands and ridges, which sets up a partial standing wave pattern with antinodes at which fracture is most likely. In the case of fast ice in bays, for instance, it is often observed (Squire, personal comm.) that the ice breaks back as far as a headland, while ice in the lee of the headland remains in place; this is presumably related to reflection (or refraction) of an incoming wave.

Finally, we cannot neglect the possibility of wave generation by wind blowing over the fast ice. This has been investigated theoretically (Mills, 1972) and observed many times, but the nature and magnitude of the wind/ice coupling are not known, and so the possible extent of ice breakup by this method cannot be estimated.

(ii) Breakup by ice edge waves. By an "ice edge wave" we mean the local wave components that represent the complex solutions to eqn. (2). Wadhams (1973b) analyzed the propagation of wave energy across an ice boundary for the perfectly elastic case and found that two additional wave components besides k have to be introduced. These are complex conjugates, with complex radian wave numbers $k_1 = a + b\,i$, $k_2 = a - b\,i$. The variation of a and b with frequency has to be derived by iteration, but at the limit of long wave periods

$$a \to \frac{\rho_w g}{4L}, \quad b \to a \qquad \text{as } T \to \infty \tag{3}$$

Thus for a given ice thickness the "wavelengths" of these components do not depend strongly on wave frequency and tend to a constant value at long periods. The physical effect of the components is to introduce a diagonal standing wave at the ice/water boundary plus a decaying progressive wave which becomes negligible beyond one wavelength. These components combine to yield a maximum bending of the ice which is greatest at a distance of some 15-30 m from the ice boundary, being slightly greater than the maximum bending due to the normal progressive wave. In a uniform ice sheet, therefore, the ice will tend to fracture at this position. Squire (1979) carried out a more rigorous analysis based on a viscoelastic model, and Figure 4 shows an estimate of how the amplitude of ice strain varies with distance from the ice edge.

This effect will tend to cause erosion of the ice edge with ice breaking along fracture lines parallel to the ice edge and separated by 15-30 m intervals. This is precisely what has been observed with bay ice in northern Newfoundland (Figure 5, from Squire, 1979). In this figure the separation of the fracture lines is about 20 m. The effect cannot be important in the large scale breakup of fast ice, but is important as a local effect. The observations show, as predicted by theory, that the crack separation does not vary strongly with period, waves varying from 6 s to 14 s causing the same pattern of fractures.

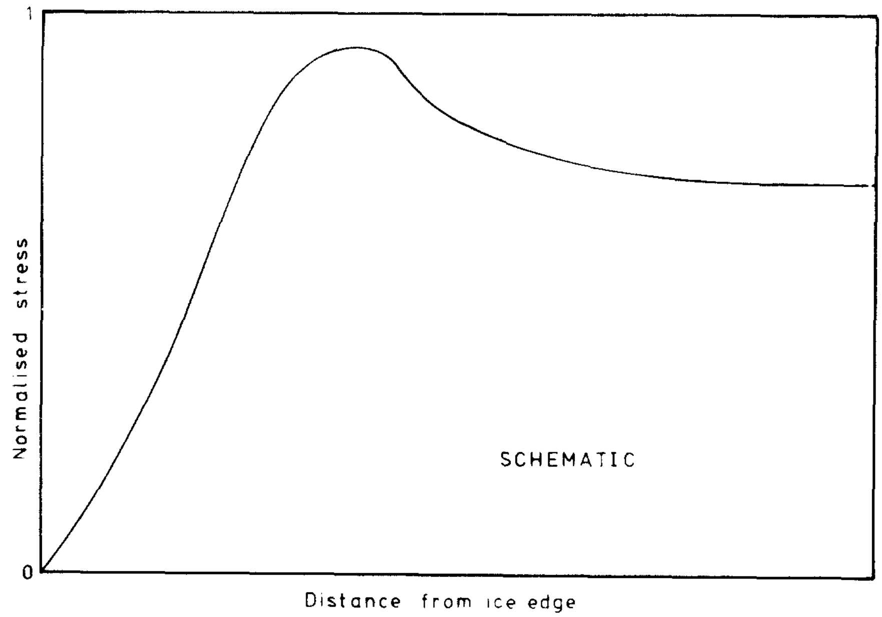

Figure 4. Schematic Diagram of stress magnitudes near an ice edge due to waves.

(iii) Breakup by wind or water stress. Apart from wave generation by wind there is the direct effect of wind stress on the ice surface. In the absence of pressure ridges the wind drag on fast ice is almost entirely flat-plate drag and so is given by (Banke et al., 1976)

$$\tau_w = C_{10} \rho U_{10}^2 \qquad (4)$$

where U_{10} is the wind at anemometer height, ρ is air density and C_{10} is the surface drag coefficient, of the order of 1.7-2.1 x 10^{-3}. This stress generates a tilt in the downwind direction, which has been measured on the moving pack of the Beaufort Sea (Weber and Erdelyi, 1976). The tilt in turn causes a combination of tensile and shear stresses in any cross-section of the ice sheet, which may become large enough to fracture the ice. Weeks and Assur (1967) reviewed the then available information on tensile and shear strengths, finding the latter more limited. A more recent review (Weeks, 1976) came to the same conclusion. A full analysis is needed of the effect of wind or water stress on a uniform ice sheet which is bounded at one end (the shore) and with a free water boundary at the other. This would determine whether such stresses can be a major cause of breakup and, if so, what wind/ current velocities are necessary.

Crystal Axis Orientation in Fast Ice

The crystal structure of fast ice sheets, and of ice sheets in general, has been described by Pounder (1965) and Weeks and Assur (1967), and is well known. Except where very rough water

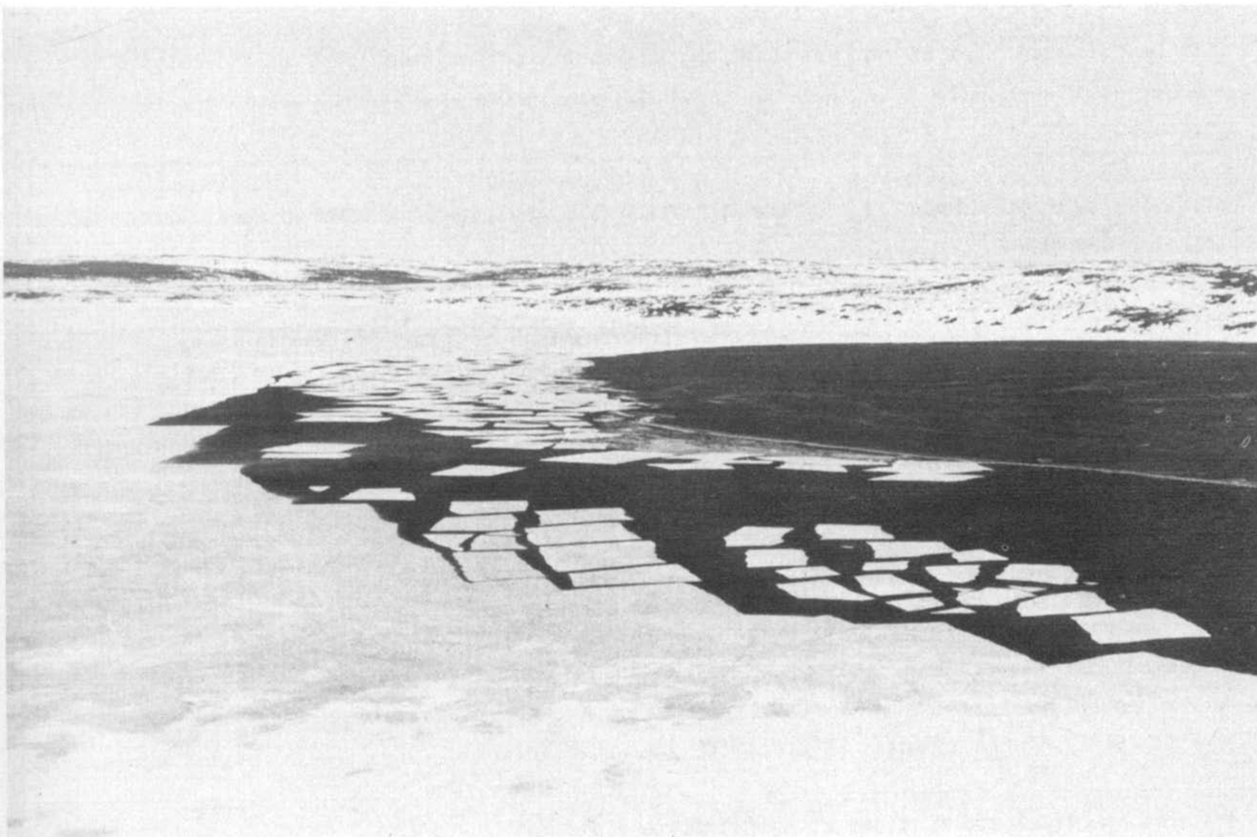

Figure 5. Breakup of bay ice in St. Anthony Bight, Newfoundland (after Squire, 1979).

has been involved in its early growth, the ice sheet shows an upper transition layer with small, randomly oriented crystals. As the depth increases, the structure is increasingly taken over by vertical columnar crystals with horizontal c-axes. The explanation is that a geometrical selection process has been taking place; crystals grow more easily parallel to the basal plane, where new molecular sites are more readily available, and so crystals with horizontal c-axes grow downwards rapidly and "take over" the whole of the ice-water interface from crystals with c-axes at other orientations.

Until recently it was thought that although ice sheets have horizontal c-axes, the actual orientation of the c-axis in the horizontal plane is random. Recently this was found not to be so in the case of fast ice. Weeks and Gow (1978) found that ice samples from the Alaskan fast ice all had pronounced horizontal orientation of the c-axes in the lower part of the sheet and their results were confirmed by Kovacs and Morey (1978) and by laboratory experiments still in progress (P. Langhorne, personal comm.). Their observations were that:

(i) The c-axis orientation develops more slowly than the columnar crystal fabric itself (typically columnar crystals begin after 15 cm, but pronounced horizontal orientation only after 50 cm);

(ii) In the lower part of the ice sheet the horizontal orientation is so well developed (standard deviation less than 10^{0}) that the ice sheet as a whole would behave as a very large single crystal;

(iii) The c-axis alignment is in the direction of the long-term mean surface current at the location concerned.

Observation (ii) explains the results of Campbell and Orange (1974) on the directional dependence of the electrical properties of sea ice. The most significant result is (iii). C-axis alignments have been reported before, by Cherepanov (1971) in the Kara Sea, but ascribed to the effect of the Earth's magnetic field. There is no known mechanism by which this could generate such a strong alignment; instead currents seem the most likely hypothesis, as they fit Weeks and Gow's results and can also be made to fit Cherepanov's results, although some of the latter's data were obtained from moving pack in the Kara Sea rather than fast ice. It is supposed that this moving pack was actually quasi-static in the same way as parts of the Beaufort Sea pack are in winter. The mechanism of alignment by currents is not known. It must be a geometrical selection process which acts to favor c-axes oriented in the current direction, but a proper physical explanation will depend on a careful analysis of the thermodynamics and hydrodynamics of the boundary layer at the ice/water interface.

The practical applications of this discovery are:

(i) Long-term currents can be inferred from axis orientations in sea ice cores.

(ii) Sea ice which originated as fast ice can be identified. For instance, the very thick (12 m) floe on which the Soviet station SP-6 was established in 1955 must have originated as fast ice, since Cherepanov (1964) reported extensive c-axis orientation in this floe. Presumably it began life as a "plug" of fast ice in a channel in one of the Soviet Arctic islands, growing for several years (perhaps 40) before breaking out. Similar instances in the Canadian Arctic have been analyzed by Walker and Wadhams (1979).

THE SHEAR ZONE

In this section we shall consider mainly the classic shear zone which extends from Alaska to north Greenland around the rim of Arctic Ocean. It is here that the boundary conditions for Arctic Ocean ice drift are determined. Here in winter the Polar pack, driven by the wind pattern over the Arctic Ocean, moves against the landfast ice and becomes heavily deformed by shear and convergence, generating a zone of pressure ridging which is heavier than any occurring in the central Arctic. In fact we shall define the shear zone, somewhat arbitrarily, as the region within which the ice characteristics differ significantly from those of the central Arctic. Detailed studies of processes occurring in the winter shear zone have been limited by the harsh conditions. The two most important questions in studying the zone are probably:

(i) How does the distribution of ice thickness and ridging compare with other parts of the Arctic, and why is it different?

(ii) What is the field of motion of the shear zone, on short and long scales of time and distance? Does it approximate that of a boundary layer or is it more complex?

Ice Geometry in the Shear Zone

The shear zone begins at the edge of the fast ice, i.e., at about 20 m water depth, and extends out an unknown distance into the Arctic Ocean, possibly reaching across the continental slope into deep water before its properties merge with those of the central Arctic ice. The basic questions of geometry are; how wide is the shear zone (i.e., for what distance from shore does the ice have properties distinctly different from ice in the central ocean), and how do the ice characteristics differ from central Arctic ice?

The best answers to these questions come from submarine sonar profiles. Two recent sets of data have been gathered wholly, or partly, from within the shear zone. The first was obtained in April 1976 by USS GURNARD in the Beaufort Sea, the profile beginning at the 100 m isobath north of Barter Island (Figure 6). The track was analyzed in 50 km sections (Figure 7) by Wadhams and Horne (1978). The second was obtained mainly in the Eurasian Basin by HMS SOVEREIGN in October 1976, with 1000 km of her track traversing the shear zone north of Greenland and Ellesmere Island. Both of these profiles therefore cover the outer shear zone, rather than the inner portion at 20-100 m water depth.

Beginning with the GURNARD profile, it was found that sections 1 and 2 of the profile differed significantly from sections 3-25, which formed a homogeneous whole. Sections 26 and 27 also differed slightly, presumably because the shear zone was again being approached. We shall look at sections 1 and 2 in relation to 3-25, since these show the clearest progressive transformation of ice conditions across the shear zone:

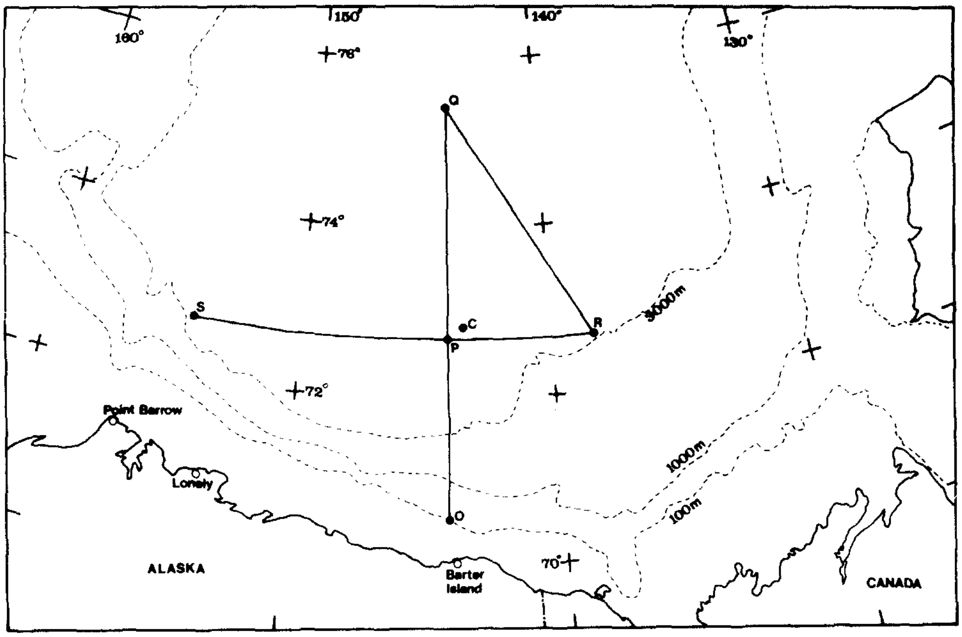

Figure 6. Track of USS GURNARD, 7-10 April 1976.

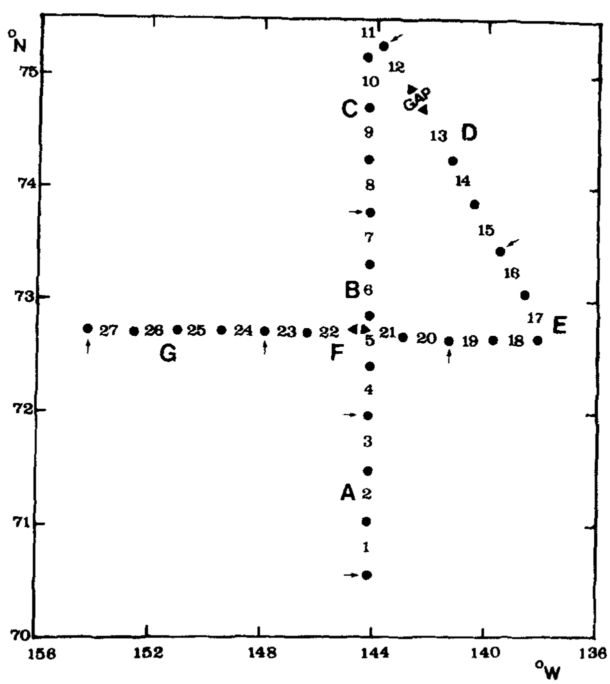

Figure 7. Division of GURNARD track into 50 km sections.

		Section 1	Section 2	Central Beaufort Sea (3-25)
Position	N	$70^{o}36'$-$71^{o}04'$	$71^{o}04'$-$71^{o}31'$	$71^{o}30'$-$75^{o}30'$
	W	$144^{o}13'$	$144^{o}13'$	138-151^{o}
ICE DRAFT	Mean	5.09 m	4.22 m	3.67 m
	Percent 0-1 m	4.5	0.8	3.5
	Percent >5 m	41	25	17
PERCENT UNDEFORMED ICE		35	44	56
PRESSURE RIDGES (>9m)	Number per km	5.1	3.1	1.4
	Mean draft m	12.2	12.2	11.8
	Maximum draft	23.1 m	28.8 m	31.1 m

The mean ice draft and percentage of thick ice (>5 m) both decline roughly linearly with increasing distance from the coast. The percentage of deformed ice (defined in a fairly arbitrary way) increases, but the most drastic change is in the frequency of pressure ridges, which is greater by a factor of 3-4 in section 1 than in the central Arctic. We note that the mean draft of pressure ridges is not significantly higher in the shear zone, but simply their frequency. Similarly, the deepest keel in the track was found in the central Beaufort Sea, although this is explained by the greater track length. Another interesting phenomenon is the occurrence of thin ice, which is generally rare throughout the shear zone except in one small part of section 1 where it reached 13%. Elsewhere the percentage is less than the average for the central Beaufort Sea, which raises the question of how the intense ridging in the shear zone can occur if there is little thin ice to provide the raw material. One could postulate that occasional intervals of divergence occur, which allow thin ice to grow for a short while between the longer intervals of compression, or else that the ridging takes place progressively as the shear zone ice moves downstream from the Arctic Archipelago towards the Beaufort Sea (i.e., that shear zone ice remains in the shear zone rather than being advected into the central Arctic), or finally that the forces of compression and shear are so great that ridges are created out of ice sheets of normal thickness rather than just thin ice. The question is unresolved.

The SOVEREIGN profile (Figure 8) ran almost parallel to the north Greenland coast for several hundred km, the closest approach being 80 km in sections 5 and 6; point B lay 180 km off the northern tip of Ellesmere Island. Very heavy ridging was observed throughout sections 1-10 (Wadhams, 1979), far heavier than in the GURNARD profile, but with a definite change in characteristics after section 5. Sections 1-5 had mean ice drafts of 6.04-6.95 m, with quite large percentages of ice less than 0.5 m thick, the figures being 1.8, 8.6, 8.0, 12.2 and 8.7 for the five sections. Sections 6-10 had distinctly higher mean drafts of 7.20-8.92 m with

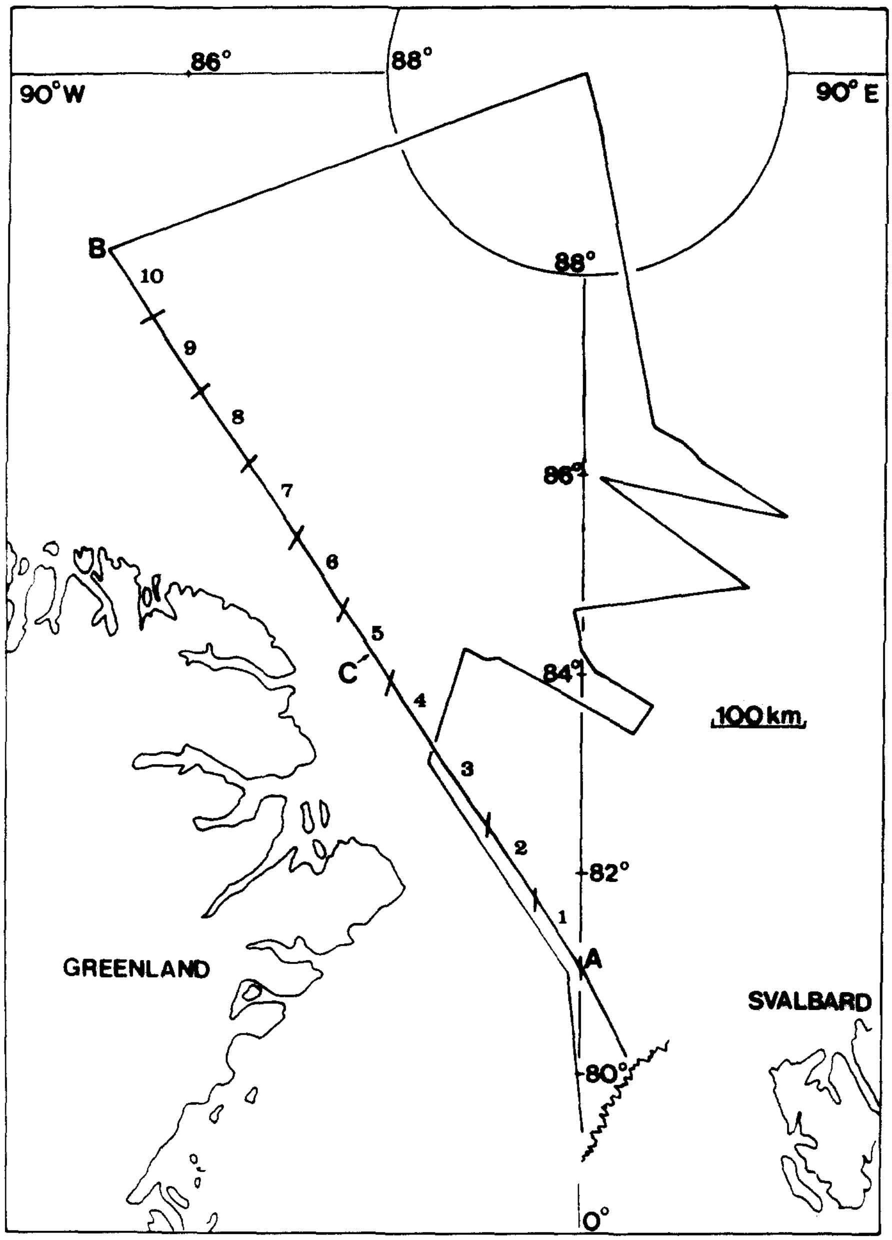

Figure 8. Division of SOVEREIGN track into 100 Km sections.

much lower percentages off thin ice (1.9, 2.0, 1.1, 2.1, 1.3). The inference is that sections 1-5 are a shear zone for ice from the Trans Polar Drift Stream coming from the vicinity of the North Pole while 6-10 are a shear zone for Beaufort Gyre ice. Numerical models of Arctic ice draft (e.g., Hibler, 1978, 1979) show this to be the case, with the area of sections 4-6 being a zone of little or no motion. Again we have the occurrence in the Beaufort Gyre shear zone of very heavy ridging associated with little or no thin ice. Even more important, further analyses (Wadhams, unpubl.) of the track running northwards from point B in Figure 8 have shown that the transition from shear zone conditions to central Arctic conditions occurs very far from the coast. Continuing in 100 km sections, we find that for a section ending at 86°45'N the mean draft is 7.63 m, for the next section (to 87°42'N) it is 6.81 m, and only in the third northward section do "normal" Arctic ice thicknesses begin (although, at 4.7-5.3 m, the mean draft is still higher than the central Beaufort Sea). This agrees with the results of an early analysis (Wadhams and Lowry, 1977) which shows a sharp decline in pressure ridge frequency and mean draft at 87°N. In other words, distinctly heavier ice ridging and thicker mean drafts are found at least as far as 87°N on 70°W, a distance of over 400 km from the coast of Ellesmere Island.

The fact that the percentage of thin ice is also high (5-7% of ice is less than 30 cm thick) between 86° and 88°N gives us a clue as to the origin of the shear zone. In the vicinity of the North Pole, ice originating from both the Drift Stream and the Beaufort Gyre is moving down towards the north coast of Greenland and Ellesmere Island. On its way, somewhere in the region 87-88°N, 60-90°W, it begins to feel the influence of the coast, transmitted as internal stress through the ice from the downstream land boundary. At this time the icefield is very open, with probably a net divergence in the east-west direction. This allows extensive ridging to take place as soon as the distance influence of the land is felt, so that even at 87°N the ice is taking on the new character of "shear zone ice". In other words, the heavy pressure ridging found in the shear zone off Ellesmere Island (the origin of the Beaufort Sea shear zone) is mainly created far out in the Arctic Ocean. There is no need, or possibility, for further extensive ridging near to the coast, so here heavy ridging and the absence of thin ice can coexist. To put it another way, the shear zone begins 400 km from land off Ellesmere Island because the ice is moving towards land, and only 160 km from land off Alaska because it is moving parallel to land. Further elaboration, or refutation, of this idea depends on the work of numerical modellers and on the constitutive equations that are found best fitted to describe the long-range drift and deformation of the Arctic ice cover.

Returning now to the inner part of the shear zone, in 20-100 m water depth, we find no direct submarine profiles and must depend on the results of airborne laser profiles. Weeks et al. (1979) and Tucker et al. (1979b) carried out an extensive program of laser profiling, with tracks running 200 km out from six starting points spaced evenly around the north coast of Alaska. From these profiles they were able to derive the distribution of the sail heights of pressure ridges. Their conclusions can be summarized thus:

(i) There is a seasonal variation in mean sail height, being low (1.1-1.2 m) in summer and early winter, and high (up to 1.8 m, all relative to 0.98 m cutoff) in late winter, i.e., February-April.

(ii) There is a similar seasonal variation in number of ridges per km, varying from 1.4-2.7 in August-December to 4.4 in February-April.

(iii) There is slightly heavier ridging in the Beaufort Sea than in the Chukchi Sea.

(iv) The largest frequency of ridging occurs at 20-60 km from the coast.
The 20-60 km distance range corresponds almost exactly to a 20-100 m depth range. Obviously in winter little ridging is seen inside the 20 m contour, since this is the edge of the fast ice zone within which the only ridges are relics of pack ice pressures during freeze-up. The 20-100 m range corresponds to the zone of greatest shear and presumably greatest deformation. This can be seen when we consider the motion of ice in the shear zone.

Clearly the heavy ridging in the shear zone implies that air and water drag coefficients used in modelling must be greater in this area.

Ice Motion in the Shear Zone

The accepted picture of the shear zone on the large scale is that of a region in which the clockwise motion of the Beaufort Gyre is gradually dissipated by a number of mechanisms until the net longshore velocity at the boundary between the shear zone and the fast ice is quite small. Many of these mechanisms generate extensive ice deformation. The velocity shear across the shear zone is therefore similar to the velocity profile in a boundary layer and can be represented by some smooth function, possibly logarithmic. Unfortunately, observations have shown this simple picture to be not entirely true.

The long-term average ice drift in winter within the Beaufort Gyre has been given as 2 to 2.5 km/day (Coachman and Barnes, 1961), and an analysis of satellite images during a single month (April) gave 3 km/day (Campbell et al., 1975). Hibler et al. (1974) carried out a satellite image analysis of how this drift rate diminishes across the shear zone, and found that, rather than being continuous, the shear all took place in a narrow zone about 50 km wide near the fast ice boundary. Beyond this the Gyre behaves as a relatively cohesive mass. These results referred only to a short period in March 1973 and may not be representative. The authors' conclusion was that the shear zone cannot be modelled by assuming a single viscosity for the ice and no slip at the boundary. Instead one should either use two viscosities (a lower viscosity applying to the region nearest the fast ice boundary) or else a single viscosity with slip allowed at the boundary. The shear zone is thus seen as something approaching a slip plane rather than being a continuous zone, in terms of dynamics if not of ice characteristics.

Tucker et al., (1979a) measured shear zone drift velocities directly using radar transponders mounted on floes and tracked from stations on Narwhal and Cross Islands. The furthest station was 37 km seaward of the islands, i.e., 60 km from the coast, and gave the surprising result that between November 1976 and March 1977 the net westward displacement was only 5 km. Stations closer to the coast showed even lower net drifts, although cyclic displacements of 0.5-1.5 km amplitude were frequent. The displacements showed only a slow, weak response to local winds and were therefore determined by stresses from the distant pack. The authors' conclusion was that throughout the winter the Gyre was effectively stationary, exerting a net compressive force on the shear zone which prevented motion. Only during early to mid-summer is the Gyre free to move. During the periods of no motion we can scarcely think in terms of a shear zone existing at all. Again, however, their conclusions refer to a single winter, which may not be representative of normal conditions. The inference that we draw from comparing Tucker et al. (1979b) with Hibler et al. (1974) is that general conclusions about shear zone motion cannot be drawn from short-term observations, and that what is required is a long-term analysis of satellite imagery, a very laborious task but one that should be done.

The nearest approach to such a study has been a review by Reimnitz et al. (1977) who carried out an intensive investigation of the shear zone off the north coast of Alaska which combined ground observations with the analysis of airborne and satellite imagery. Their conclusions were as follows:

(i) There is a distinct inner part of the shear zone which they named the stamukhi zone (after Zubov, 1945), consisting of a belt of lineated ridges and hummocks, the deepest points of which are aground. This zone develops during early winter as the pack grinds against the fast ice zone, and is distinct from the ridged outer fast ice zone. The stamukhi zone develops further throughout the winter, constantly increasing its width as Gyre ice grinds and shears against its seaward edge and eventually becomes deformed enough to be incorporated in the stamukhi, possibly with keels gouging the bottom. Within the stamukhi zone further deformation continues to occur, with active bottom gouging taking place, and thus the stamukhi zone represents a vast energy sink.

(ii) Shear occurs intermittently either within or to seaward of the stamukhi zone, and takes place within the small compass of a few hundred m, far less than even the 50 km stated by Hibler et al. (1974). The whole shear between the "stationary" ice (ie the stamukhi zone of the inner "shear" zone) and the normal Gyre ice takes place in this very narrow slip plane, so there is no such thing as the continuous velocity shear normally postulated. The stamukhi zone extends out to about 40 m water depth. The existence of stamukhi beyond a fast ice zone that extends to 20 m is also characteristic of the East Siberian Sea (Zubov, 1945).

The picture of Reimnitz et al. (1977) is not entirely incompatible with the observations of Hibler et al., since Hibler's drift net employed a small number of identifiable floes on a 15 km grid. A large shear occurring in a narrow zone between two grid points would be interpreted as a shear over 15 km; this still does not explain the 50 km figure, however. The picture also fits Tucker et al.'s observations if we suppose that their transponder stations were in the stamukhi zone. The picture is an original one because of its implications for modelling. The winter shear zone, they say, would be modelled in the following way:

(a) Intermittently there is perfect slip along a single line between the Beaufort Gyre ice and an essentially stationary segment of the inner shear zone known as the stamukhi zone, in this case behaving as if it were fast ice.

(b) Between these periods of perfect slip there is no slip at all; the Gyre ice grinds against the stamukhi, and its energy is dissipated in bottom gouging and in the creation of new expanses of linear shear ridges and hummocks (probably by the grinding up of thick ice blocks rather than thin ice from leads).

The nearshore ice oscillates between these two modes which stand out in stark contrast to one another. In (a) there is no shear zone and perfect slip. In (b) there is no slip but heavy energy loss. In the case of (b), is there some kind of continuous velocity shear further out in the outer "shear zone"? In other words, do the times when the Gyre ice is grinding against the stamukhi always coincide with the times when the whole Gyre itself appears to almost stop moving (as it did during the AIDJEX experiment)? If so, then there is never a shear zone in the accepted sense of the word. If not, then there presumably is a shear zone, ie a continuous velocity shear, but it lies further out to sea, in the outer part of what we have labelled as the shear zone in terms of its ice characteristics but which was originally named the offshore province by Weeks et al. (1971). This would allow ice deformation and ridging to occur out to the 160 km distance found from submarine observations, while still leaving the stamukhi-grinding as a significant energy-dissipating effect which should be included in modelling studies.

The Flaw Lead and Other Open Water Areas

A feature of the shear zone throughout its length, including the portion that lies off Greenland, is the intermittent existence of a wide lead which separates the moving ice from the fast ice or apparently fast ice. This is the flaw lead, which exists in winter as well as in spring, when it forms the nucleus for a system of leads which expands into areas (e.g. Amundsen Gulf) which are later to become ice-free. The existence, or otherwise, of the flaw lead is clearly dependent on the overall Arctic ice dynamics. When the overall wind stress acts to move the ice away from the coast the flaw lead opens; when the stress is against the coast it closes. It may be that the flaw lead corresponds to the slip line described earlier, so that the "stamukhi zone" is left on the shoreward side of the lead when it opens. Any model of shear zone dynamics has to be able to explain and possibly predict the opening of the flaw lead. As we shall see in the next section, given the correct wind stress field as input most models will correctly predict a great decrease in compactness or viscosity near the land margin, but no model has been constructed which is capable of predicting the opening of a specific lead. This is because the small-scale effects which cause a single large lead to open rather than a series of leads (i.e. the existence of grounded ridges inshore) are not included in the model. Figure 2 shows a flaw lead in April.

A similar phenomenon to the flaw lead is the winter polynya, a few of which exist as semi-permanent entities on well-defined coastal areas of the Arctic. The best known is the North Water in Smith Sound, but there are others off north-east Greenland and in the Soviet Arctic, as well as many in the Antarctic. The cause is the combination of a strong prevailing wind with a fixed upwind boundary (usually land or fast ice) and no downwind boundary, so that new ice is advected away as fast as it forms. Such polynyas act as ice factories throughout the winter, and are areas with greatly increased vertical heat flux and evaporation.

Another phenomenon of interest is the occasional observation of spatially periodic lead patterns in the Beaufort Sea, of which the flaw lead forms the southern limit. The pattern is an intersecting mesh formed of two sets of parallel leads spaced 100 km apart and was first explained as a consequence of the existence of planetary waves (Marko and Thomson, 1975), although this explanation was later withdrawn in favor of one based on semi-brittle failure (Marko and Thomson, 1976). A related phenomenon is found in the Chukchi Sea where, if a southward ice drift should occur, the land boundaries form a converging throttle. This produces a mechanical effect on the ice similar to the pattern of failure of wet sand in a hopper, and Sodhi (1977) has presented some beautiful satellite images showing this effect in the Chukchi Sea and Amundsen Gulf.

Modelling of Shear Zone Dynamics

To date modelling of shear zone ice dynamics has consisted of modelling the whole Arctic Ocean, or at least a large part of it (e.g. the AIDJEX model), and then considering the results for the grid elements which lie closest to the coast. Since in all of these finite difference schemes the grid size is at least 100 km the results can only give a coarse picture of the shear zone, the whole thickness of this zone being represented by a single grid element. On the other hand, since the motion in the shear zone depends greatly on internal stress transmitted from distant parts of the pack, it is difficult to see how the shear zone could be modelled in isolation. Since the grid size is mainly determined by the present capacity of computers, we cannot expect a radical improvement in shear zone modelling in the near future. The important question to ask is: are modelling schemes correct in assuming that the shear zone follows the same laws as the central Arctic, or are there important processes going on in the shear zone which are not included in models and which therefore make whole-ocean models inappropriate for dealing with the shear zone?

A typical whole-ocean model applied to the shear zone is that of Hibler (1978), which uses a one-day time step and 125 km grid. The model is "driven" by thermodynamic seasonal growth rates given in Thorndike et al. (1975) as a function of ice thickness, and by geostrophic wind fields derived from surface pressure data obtained over a year. By running a simulation over four "years" results were obtained which were reproducible for a given day of the year. The momentum equation is a normal balance of Coriolis force, wind stress, water stress, internal ice stress, ocean tilt and acceleration. The constitutive equation for ice properties is a viscous-plastic law which is plastic at normal deformation rates and viscous at very small rates. The plastic strength P is modelled as a function of compactness A (fractional ice cover) and thickness h by

$$P = P' \, h \exp C\,(A-1) \qquad (5)$$

where $P' = 10^4$ N m^{-1} and $C = 20$. The behavior was found to give a good approximation to observed phenomena in the shear zone, especially in summer.

The AIDJEX model has also been applied to the shear zone (Pritchard et al., 1977; Pritchard, 1979). This employs an elastic-plastic constitutive law for ice properties. Application of the model to a period of 8 days during which concurrent observations from manned camps and buoys were available showed realistic agreement, and even when a large flaw lead occurred in the shear zone the ice velocities agreed well. Other sea ice drift models also generate a shear zone with typical shear zone properties. A model by Sodhi and Hibler (1979), for instance, can be forced by a given distribution of tidal current velocity to give the resulting sea ice drift in a constricted channel (Strait of Belle Isle); it is clear that this has a possible application to the shear zone.

To summarize, most models of ice dynamics that reproduce the major patterns of Arctic Ocean ice drift satisfactorily also generate a shear zone with reasonably realistic properties. This seems to happen regardless of the precise constitutive law chosen, and the variable that seems to have the most effect is the choice of slip or non-slip boundary conditions around the margin with land. Perhaps a new boundary condition should be tried which fits the field observations of Reimnitz et al. (1977), although for this to reproduce the finer structure of the shear zone the grid size of the model will have to be greatly reduced.

Ice Scour

Linear gouges of the sea bottom in shallow water have been reported and extensively mapped in the Beaufort Sea off Alaska (Reimnitz and Barnes, 1974) and off the Mackenzie Delta (Pelletier and Shearer, 1972); Shearer and Blasco, 1975; Lewis, 1975). The gouges are generally 0.5 to 1.0 m deep, but some are as deep as 5.5 m. The gouge density is greatest in the water depth range 10 to 30 m, sometimes exceeding 100 per km of survey track, but gouges have been observed in water as deep as 100 m. The gouges are generally narrow, indicating generation from grounding pressure ridges, but a few are wide features with multiple striations, indicating the effect of a grounding ice island fragment.

Neglecting ice islands, a quantitative explanation for the present distribution of scours requires knowledge of three parameters:
(i) The present (and past) distribution of pressure ridge keel drafts at the location concerned, such as a point (x,y,h).
(ii) The present (and past) mean annual ice drift past (x,y,h).
(iii) The history of submergence of (x,y,h) over the past few thousand years.
Geological factors are involved because much of the Beaufort Sea shelf has been sinking since the last glaciation, as part of a general tilting of the North American Shield following removal of the continental ice sheet. A point (x,y,h) on the seabed therefore was formerly (x,y,h') where $h'<h$, so that in the past it would have received more frequent gouges than it does at present. The rate of sedimentation on the shelf is less than 1 m per 1000 years, so

that scours at least 1000 years old will still be visible today; therefore an integration over time and a depth range is necessary to obtain the present scour density at (x,y,h).

We can ignore geological factors if we confine ourselves to the problem which is of practical importance to those who seek to perform operations on the seabed such as wellhead completion and pipeline construction. This problem is just the present rate of scouring, which requires knowledge of only the present values of parameters (i) and (ii). It is clear that the scour distribution can be explained qualitatively in terms of these parameters. The density is low at water depths below 10 m because a consolidated sheet of fast ice covers this area for at least 8 months per year, so that ice can only drive ashore in the summer; further, the bottom at such shallow depths is subject to considerable reworking by the sea. The density falls off beyond 30 m because the pressure ridge frequency beyond this draft is very small, more than making up for the greater annual ice drift rate: the deepest pressure ridge yet observed had a draft of 47 m (Lyon, 1967), followed by a 43 m keel (Wadhams, 1978a). Between 10 m and 30 m there is an optimum product of drift rate and keel frequency. If P(h) is the probability density function of keel draft, N is the mean number of keels per km and S km is the mean annual drift rate, then the annual rate of deposition R of new scours at the point (x,y,h) is

$$R = N\,S \int_{h}^{\infty} P(Z)\,dz \qquad (6)$$

Assuming that S is known, R can be found from the keel draft distribution. The problem is, of course, that no direct measurements of keel draft distribution can be made (by submarine) in such shallow water. One could envisage the use of a small submersible or unmanned vehicle (Francois and Nodland, 1972) to carry out this task, but in their absence we must either use submarine data from deeper water (e.g. the track of USS GURNARD, Wadhams and Horne, 1978) or else make inferences from airborne laser profiles of sail height distributions. The latter course was attempted in Wadhams (1976) and Weeks et al. (1979). Wadhams simply used a multiplication factor of 3-4 to convert sail heights to keel depths, but since then a better technique has been evolved based on the joint analysis of simultaneous laser and sonar profiles (Wadhams, 1979). Using this technique, P(h) can be derived from the corresponding probability density of sail heights. Such a method could immediately be applied to the laser data of Weeks et al. Weeks et al. themselves recommended an extreme-value technique which does not depend on knowledge of the analytical form of the probability density function. This could be applied if sonar data were directly available, but it is not necessary if a conversion technique is used, since this assumes a form for the keel draft distribution.

THE MARGINAL ICE ZONE

Physical Processes Associated with the Ice Margin

Ice in the area close to an open ocean margin has properties quite different from central Arctic ice. The complexity of its structure is clear from the following description by Kozo and Tucker (1974) of ice in the Denmark Strait observed in March:

> The ice pack from the edge to 56 km inside was composed of uniformly distributed small ice forms categorized by floe diameter. These included pancake ice (0.3 - 2 m across), ice cakes (1.8 - 20 m across), and small floes (20 - 100 m across). Stages of ice development ranged from new to multiyear ice, the frequency and size of multiyear ice fragments increasing inward from the ice edge. These fragments ranged from 3 m across at the ice edge to 41 m across at a distance of 56 km inside. Toward the edge the ice field was unconsolidated, but deeper inside the predominant features were angular fragments of multiyear and thick first-year ice cemented together (breccia) by thin first-year and young ice. The ice composition suggested recurrent destructive activity in this area as evidenced by small fragment size, open fractures, and very thin ice areas.

This complex structure is the result of a number of processes which occur in the marginal zone, and which we shall now consider. To fix ideas we shall think especially of a margin in which there is a mean ice drift parallel to the ice edge (Figure 9). This corresponds most closely to the East Greenland or Labrador Currents.

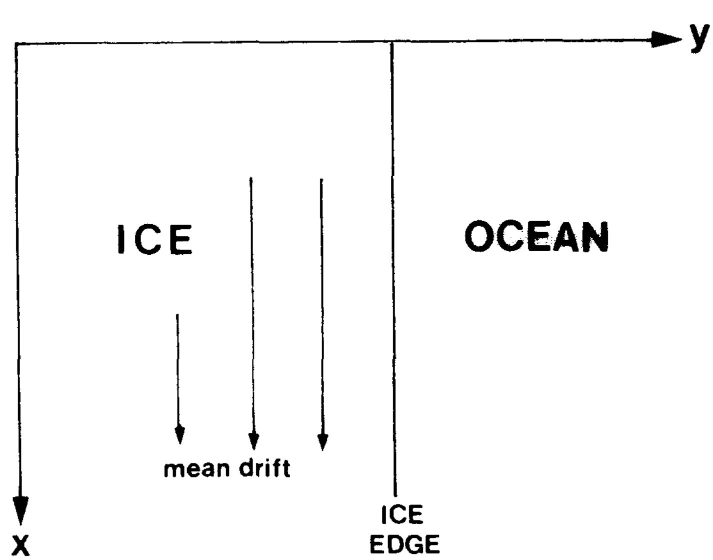

Figure 9. Schematic diagram of a marginal ice zone.

Wave-induced ice breakup

The ice in the marginal zone bends in response to incident waves and swell from the open ocean, and if the bending strain is too great the ice will break. The propagation of waves through fast ice has been considered earlier, and in the MIZ it sometimes happens that very large areas on continuous ice sheet approach the ice margin. Under these circumstances waves will propagate through the sheet in the manner described in the section on wave propagation and the equations of propagation of a flexural-gravity wave will determine whether the ice is fractured by this process. If y_0 is the amplitude of the wave in the ice and λ_0 is its wave-length (given by eqn. 2), then the maximum strain ϵ_{max} at the floe surface is

$$\epsilon_{max} = 2\ h\ y_0\ \pi^2\ /\ \lambda_0^2 \tag{7}$$

and this will induce fracture if

$$\sigma_f = E\ \epsilon_{max}\ /\ (1-\nu^2) \tag{8}$$

Here E is Young's modulus, ν is Poisson's ratio and σ_f is the flexural strength, which is typically 0.3 MN m^{-2} although it varies widely with floe thickness and salinity (Weeks and Assur, 1967; Goodman, 1977). The flexural strength is also reduced by the presence of large cracks in the ice (Parmerter, 1975) and is probably dependent on the density of small pre-existing cracks nucleated at the boundaries of brine cells. Putting in typical numbers, we find that a 9s wave requires an amplitude of 5cm to crack 2m-thick ice, while a 16s wave requires 25 cm. The amplitude of a wave in ice is less than its "open water" amplitude because of the change in propagation characteristics (Wadhams, 1973b) and the corresponding "open-water" amplitudes are 15 cm for 9 s and 30 cm for 16 s. Since the 9 s wave is attenuated much more rapidly than the 16 s wave in the broken icefield near the ice edge we conclude that the longest swells are the most effective agents for causing breakups of continuous ice sheets deep within the pack.

The normal state of ice in the MIZ is to be already broken into finite, if large, floes. In the East Greenland Current, for instance, the divergence associated with the acceleration of the current with increasing colatitude (Einarsson, 1972) will open up leads, and the funnelling of ice through Fram Strait causes patterns of leads to open due to the constraints induced by the coastline. Thus, even in the absense of waves, we still expect the ice cover to be composed of large floes (or of frequent leads, which is the same thing).

Now an independent floe of finite diameter has a rigid-body response to a wave field, with components of surge, heave and pitch. These responses relieve the bending stress on the floe, so that for a given wave frequency the wave height required to cause fracturing increases as the floe diameter decreases and is at all times greater than that given by (7) and (8). The necessary wave height is also, of course, a function of thickness and failure strength of the ice.

As waves propagate through the icefield from the open ocean they are themselves scattered and attenuated by the ice floe distribution which they have helped to set up. Studies of wave attenuation in sea ice (Wadhams, 1973b, 1975) have shown that the primary mechanism for loss of amplitude from the advancing wave is scattering by ice floes, which is a function mainly of the ratio of floe diameter to wavelength. The scattered victors then lose energy by turbulence and wave breaking around floe edges, and there is an additional large amplitude loss at the outermost edge from the same cause and from floe-floe collisions. These processes are a major source of underwater noise (Diachok and Winokur, 1974). The theoretical studies, together with measurements from shipborne wave recorders (Robin, 1963), submarine sonar (Wadhams, 1972, 1978b) and airborne laser profilometers (Wadhams, 1975), have established that the attenuation is exponential, of form

$$E(x) = E(0)\ \exp\ (-2\alpha x) \tag{9}$$

with α varying approximately as (frequency)^2. Thus only the longest period swell propagates more than a few km into the ice, and so wave-induced breakup is most effective in ice margins exposed to a long fetch of stormy sea (i.e. Norwegian Sea and Southern Ocean). A typical "skin depth" ($1/\alpha$) for a 13 s swell in a compact icefield is about 14 km and for a 16 s swell would be about 21 km. A 16 s swell of 5 m initial amplitude, from an intense storm, is reduced to 30 cm amplitude (shown by equation 8, to cause breakup of a large floe) in 3 skin depths, i.e. 63 km. This is then roughly the width of the active layer of the MIZ, within which ice breakup occurs during storms.

If an icefield were static, a steady-state distribution of floe sizes would be set up by this breakup process. The ice at the very ice edge would be broken by the large local wave field into small floes. Ice slightly further from the margin is partially protected by this fringe of floes, and the milder wave field permits larger floes to exist. Thus the maximum and average floe sizes should increase with distance from the ice edge until eventually the point is reached where waves cannot break floes at all, when infinite floe size becomes possible. Satellite and aerial photographs (e.g. Figure 10, a Landsat image) clearly reveal the outermost fringe of small floes, but the gradation to large floes is not continuous, and frequently banding is seen with secondary belts of small floes sandwiched between belts of large floes. It is clear that the floes, with their increased freedom of movement, are responding to the wind in a constant churning motion (ie. a fluctuating y-component to a mean drift in the x-direction) which advects large floes into the perilous region of the margin. Therefore the margin can be thought of as a factory, or rather a scrapyard, which pulverizes any large floes which venture into its sphere of influence. The rate of pulverization depends not only on the wave climatology of the nearby open ocean area but also on the statistics of the y-component of ice drift. In this respect studies in which floe trajectories are plotted from successive

Figure 10. Landsat image of ice edge in East Greenland Current.

Landsat images (e.g. Vinje, 1977) are especially valuable in determining the rate at which large floes enter the MIZ from deeper within the pack.

Recent observations of the ice margin in the Bering Sea, composed of thin ice between 0.3 and 1 m thick, bear out the above description with a single difference (V. A. Squire and S. Martin, personal comm.). The outermost zone of the ice field (2-4 km) was found to be composed of ridged and rafted floes 10-20 m in diameter, the wave steepness being sufficient not only to fracture the floes but also to cause direct rafting of the thin blocks. There followed, as expected, a 10-20 km zone of small cracked floes and then a zone of very large floes after the wave energy was reduced to below the limit for fracture. In my view, the necessary tasks in determining the rate and overall significance of wave-induced breakup are:

(i) To determine the total bending response and the fracture criterion for a flow of given diameter and thickness to a monochromatic wave. An experimental project to attack this problem is at present under way at Scott Polar Research Institute, Cambridge (Allan et al., 1979; Wadhams, 1979b).

(ii) To develop techniques of using wave climatology data to predict the frequency of breakup events. A first approach to this was carried out by Keliher (1976) to account for break-outs of ice from the Antarctic margin.

(iii) To understand the statistical response of an icefield, composed of independent floes of varying sizes, to a fluctuating wind field. In other words, what are the internal stresses in this kind of icefield and do they determine the mean flux of ice across a y=constant line, or can we model the floes as moving independently under an updated version of Zubov's law?

Loss of ice across the ice edge

Given that the the ice margin is a pulverization factory, what happens to its products? Obviously some are advected back deeper into the ice pack, as can be seen from photographs, although it would be interesting to analyze available imagery to see how far into the pack such belts of small floes are detectable. However, with an off-ice wind, floes can be advected in the other direction, that is out into the open ocean. This is an important process, as it represents a lateral leakage of mass from an ice drive current which may be significant enough to merit parameterization in a model of such a current. The motion of the floes often seems to occur in bands or streamers, (Figure 10a) which Muench and Charnell (1977) ascribed to atmospheric roll vortices. The bands appear parallel to the wind when close to the ice edge and perpendicular to it further out; the reason for this is not known. If the ice edge corresponds roughly to the Polar Front separating polar surface water from water some 3-4°C warmer, then the ice which is blown away from the edge will melt rapidly. The response of the ice at the edge to such an off-ice wind is quick because of the small floe size; also in the case of thin rafted blocks, because of high wind drag.

At all times ice advection away from the edge is opposed by the radiation pressure of the wave field. The directional spectrum of the wave field just outside the ice edge is directed towards the ice, and Longuet-Higgins (1977) showed that for normal incidence of waves in deep water the force per unit length on the ice edge is given by

$$F = 1/4\rho g\ (a^2 + a_1 2 - b^2) \qquad (10)$$

Figure 10a. Bands and streamers outside ice edge. Photographed from 1300 m, Labrador Sea, February (by courtesy of A. M. Cowan).

where a, a_1 and b are the incident, reflected and transmitted wave amplitudes respectively. Thus this force varies between zero and 1/2 $\rho g a^2$, where ρ is the water density, and always acts to maintain the compactness of the ice edge. In the absence of a local wind the radiation pressure can maintain a surprisingly well-defined ice edge, which appears as a single line in satellite photographs (Figure 10) and even to the naked eye when close up (Figure 11). When an off-ice wind breaks up the ice edge the radiation pressure term must be added to the balance of forces on a single floe which determines its motion.

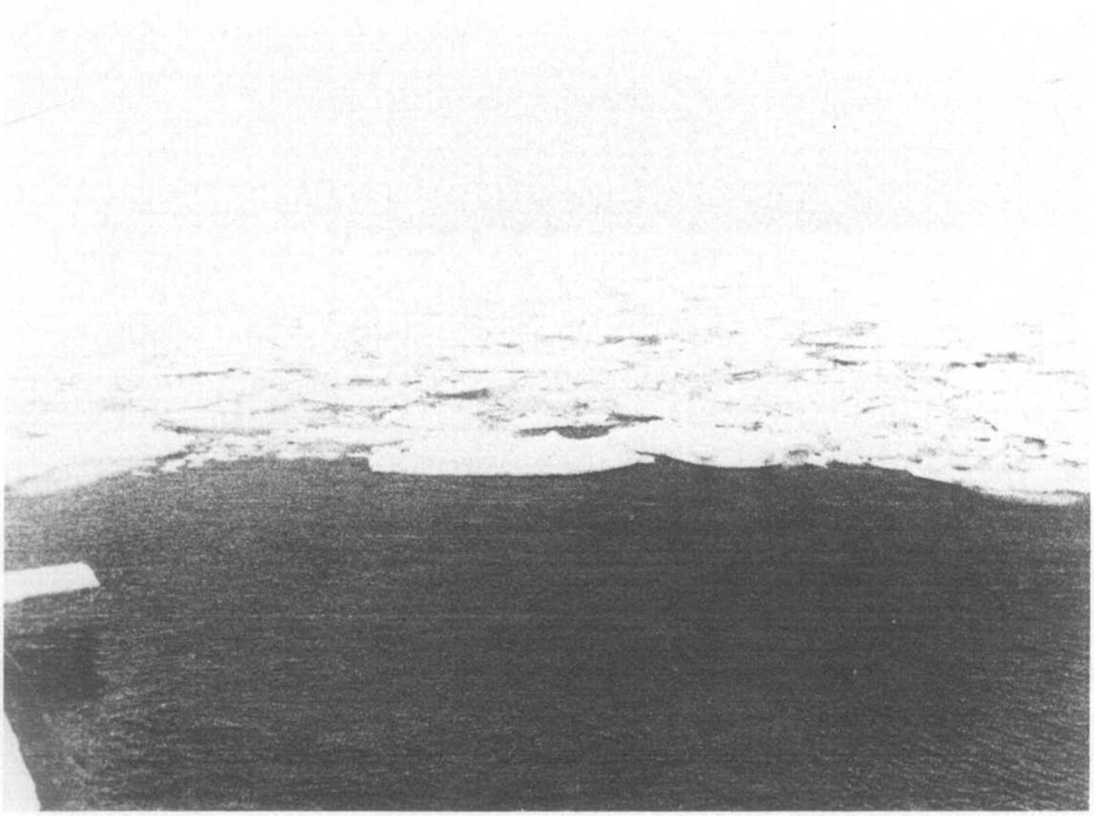

Figure 11. A compact ice edge at 80°N 3°E, February 1971. Nearest floes are 20-30 m wide (after Wadhams, 1978b).

Heat and mass transfer associated with eddies

Patches of warm water have been observed well within the Polar Front in the East Greenland Current (Wadhams et al., 1979). Figure 12 shows one such occurrence at about 79°N, in which the temperature structure is shown by a sound velocity profile obtained by a submarine while the submarine's sonar gave a profile of the overlying ice cover. The Polar Front at 85 m depth lies about 30 km to the west of the ice edge, on account of the slope of the Front caused by the velocity shear across it. Within the Polar Front, some 40 km and 80 km further into the ice, lie two warm water patches (shown by high sound velocity). It is possible that these are limbs of a large baroclinic eddy, especially as such an eddy has been observed in this part of the Front using Landsat imagery (Vinje, 1977, Figure 10). Similar eddies have been seen along the edge of the Labrador Current using satellite thermal infrared imagery (Legeckis, 1978), along the Polar Front in the Barents Sea using CTD profiling (Johannessen and Foster, 1978) and

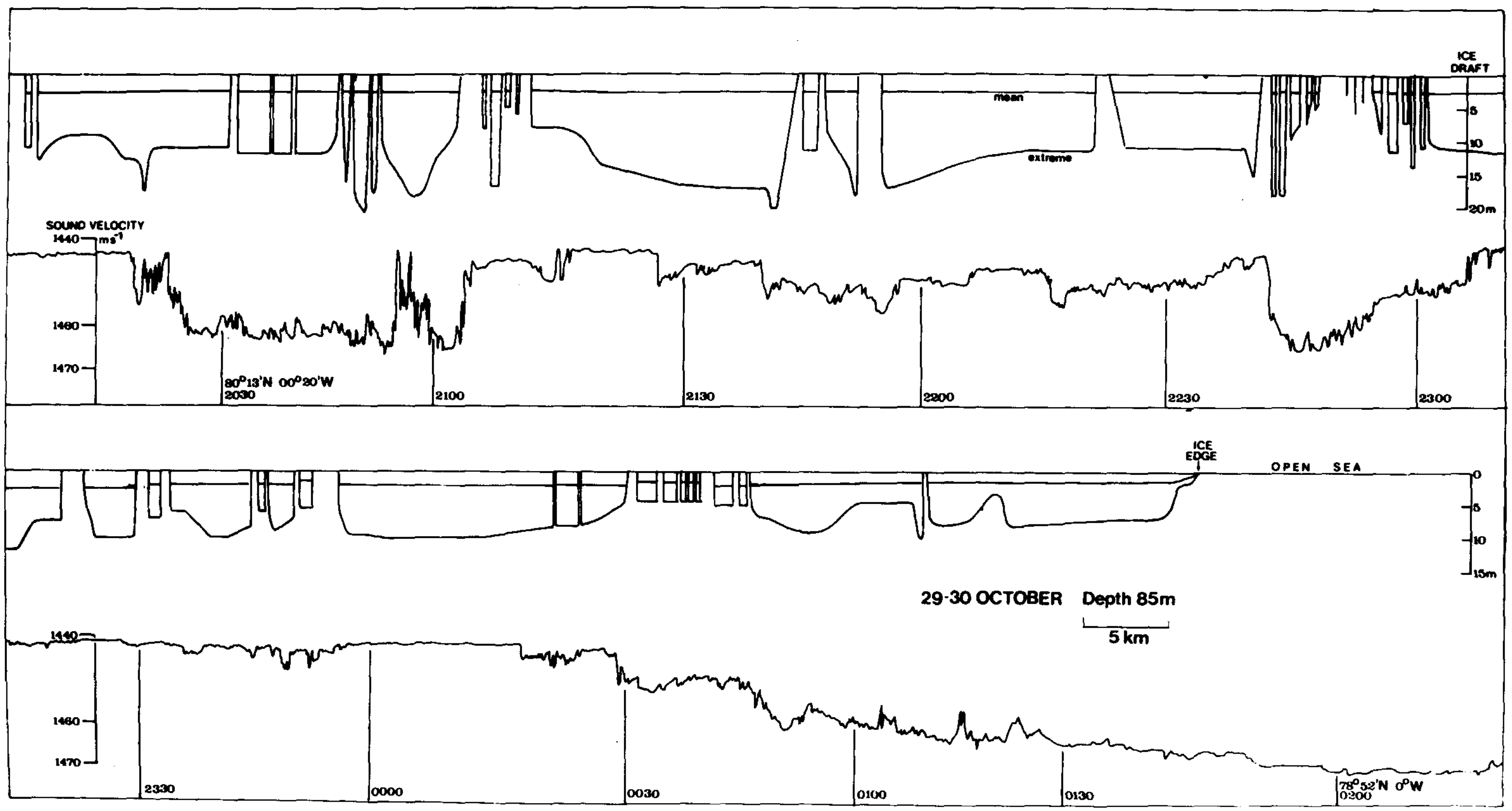

Figure 12. Sound velocity profile obtained under East Greenland Polar Front, October 1976, with associated ice draft distribution (after Wadhams et al., 1979).

along the Antarctic Polar Front (Neal and Nowlin, 1979). Theoretical studies (Jones, 1977) predict that the East Greenland Polar Front is unstable along its entire length, so that such eddies may exist along any part of the Front. There are no data available on the frequency of occurrence, lifetimes, structure, development or energies of such eddies, however. An eddy of the type seen in the Landsat image may cause loss of ice from the marginal ice zone in two ways:

(i) directly, by drawing a large expanse of ice out into the warm water zone, where it melts;

(ii) indirectly, by drawing large floes from deep within the ice pack out towards the margin, where they are broken up by waves - i.e., by increasing the rate of production of the pulverisation factory.

Figure 10 shows how, in the vicinity of the eddy, the large floes are being drawn further out towards the margin.

The development and decay of the eddy involves mixing of water masses between the Polar and Greenland Sea surface waters which causes an unknown but possibly significant heat transfer into the East Greenland Current. Eddies are thus a way in which the barrier which the Polar Front normally presents to lateral heat flux may be broken down. The magnitude of this effect can only be determined by surveying the occurrence and life histories of eddies along the ice margin, both from satellite imagery and by direct shipborne measurements.

Lateral melting of floes

We have already seen that in the East Greenland Current there is a net divergence in the ice drift, allowing leads to open up, and how throughout the MIZ ice breakup is continually in progress due to wave penetration and the increased response of the unrestricted icefield to wind action. Thus the typical ice scenery in the MIZ consists of floes, large and small, separated by an interconnecting net of channels containing open water or new ice.

If an icefield is composed of floes all of one diameter d, the total length of floe perimeter per unit area of icefield is roughly (π/d). As d decreases, i.e. as the ice margin is approached, the perimeter increases by a large factor. In summer this increases the contribution made by lateral melting to the overall melt rate. Lateral melting is an especially efficient process because:

(i) the topmost 1-2 m of water, in calm conditions, are warmer than the underlying water because of the absorption of solar radiation;

(ii) turbulence and wind-wave motion around the boundary increase the melt rate (although wind mixing negates the effect of (i));

(iii) a floe usually contains weak layers into which water can penetrate, destroying the structure from within.

It is possible that the lateral melt rate dominates the bottom and top surface melt rates in summer near the ice margin. For instance, Alekseev and Buzuev (1973) observed lateral melting of ice in a lead near the NP-16 station and estimated that 75-90% of solar radiation absorbed by the lead was used for lateral melting. The theory of lateral melt rates was developed by Zubov (1945) and is given by Doronin and Kheisin (1977).

Wave-induced melting

Near the ice margin the penetrating waves and swell generate an oscillating shear current at the ice-water interface which increases the melt rate. The magnitude of the effect was estimated by Wadhams et al. (1979), and Figure 13 shows their estimates for the time taken to melt a floe of 3 m thickness, given various assumptions. The four sloping lines are melt times due to 10 s and 13 s waves of 1 m and 5 m initial amplitude at different distances inside the

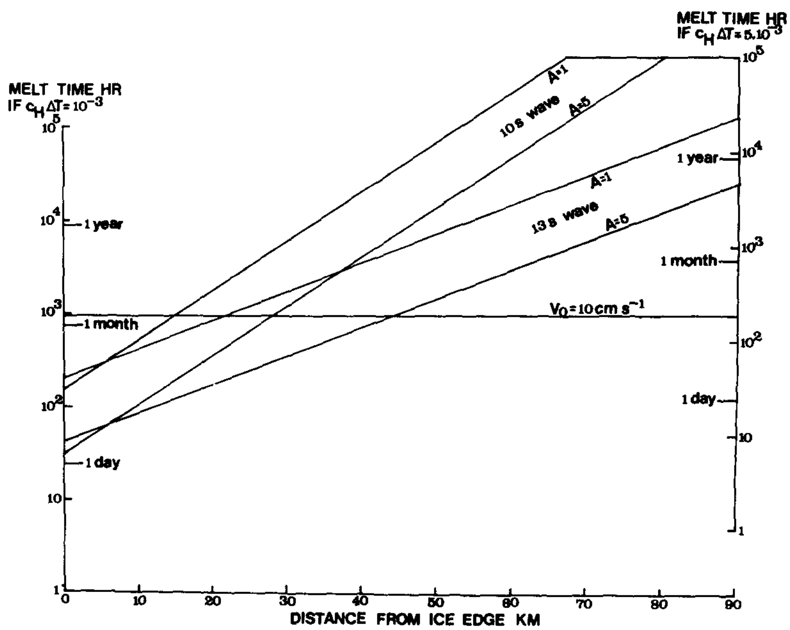

Figure 13. Melt times for a 3 m thick floe due to wave action at different distances inside the ice margin (after Wadhams et al., 1979).

ice edge. The horizontal line is the melt time for a steady shear current of 10 cm s^{-1}. The two time scales are for two possible values of $c_H \ \Delta T$ where ΔT is the temperature difference between water and ice and c_H is the dimensionless parameter found in the equation of Csanady (1972) for heat flux H across a boundary surface:

$$H = c_H \ \rho_w \ c_w \ \Delta T \ V \qquad (11)$$

Here ρ_w is water density, c_w is its specific heat and V is the shear current. c_H lies in the range 1-3 x 10^{-3}, the precise value (unknown) depending on the roughness length of the ice bottom and the degree to which an oscillating boundary layer reproduces the effect of a steady one. It can be seen that wave-induced melting dominates melting due to typical wind-induced relative drift (the 10 cm s^{-1} line) as far as a penetration of 15 to 40 km, depending on wave height and period. However, since wave decay is exponential, the wave melting effect becomes completely negligible beyond about 60-70 km. At the ice edge itself, wave melting must be very effective, especially given the small size of ice floes which increases lateral melting. The ice edge is being constantly eaten away by this process, which may well cause a mass loss greater than the simple stripping away by off-ice winds. Again, data are lacking, but the effect was well understood by Scoresby (1820) who wrote:-

> "As fast as the borders of the ice are destroyed by the sea, or the mildness of the climate under southerly winds, all the losses are made up by the prevalence of the current proceeding to the south-west, which continually brings fresh supplies of ice, and presents a new front to the action of the waves."

Geometrical Properties of Ice in the MIZ

Floe size distribution

We have seen that in the outer part of the MIZ there is a maximum floe diameter which increases with distance from the ice edge. Within the limits of this constraint, the actual floe size distribution is not known. Deeper into the MIZ, where many processes are at work together, the floe size distribution is also not well known. Most observations of floe size distribution have been made incidentally to other investigations: Dean (1966) found a negative exponential distribution in the outermost 2 km of a compact Antarctic ice margin; and Vinje (1977) found the same in a study of large floes in the Svalbard-Greenland area using Landsat imagery. If a large number of independent processes are at work, the theoretical distribution of floe sizes will be a negative exponential; this assumes that the spatial distribution of fracture events is random. Mock et al. (1972) predicted a similar distribution for the spacings of pressure ridges in an icefield using the same random assumption for ridge-building events; this gave good agreement with observations. It is clear that we must define an area scale within which a single negative exponential may describe the whole distribution of floe sizes, and this area scale is probably much smaller than the scale (50-100 km to a side) over which pressure ridge distributions are quasi-homogeneous. At the ice edge itself a given distribution may hold for only a km or less before the mean value changes radically, while the banding effect of alternating large and small floes produced by the churning motion of the icefield leads to alternating regimes with quite different parameters for the size distribution.

What is needed is clearly a proper study of flow size distributions from aerial and satellite photographs in an attempt to establish whether the negative exponential is of general validity. The resolutions of the various survey satellites range through three orders of magnitude (Nimbus 35 km; NOAA 1 km; Landsat 80 m) so that satellites are most useful for measuring floes in the medium-to-giant-size categories, leaving aerial photography to resolve small floes and cakes. It would be of great value if a negative exponential were found to hold for large floes far from the ice edge, as is suggested by Vinje, since this would offer the hope of a statistical model of ice dynamics in the MIZ being developed based on the interactions of a distribution of rigid floes, in the same fashion as the model of Solomon (1970) for central Arctic ice.

Ice roughness characteristics

For the purpose of modelling ice drift it is important to know whether the top and bottom drag coefficients in the marginal ice zone are similar to those in the central Arctic. Banke et al. (1976) expressed the overall drag coefficient C as

$$C = C_{10} + 1/2\ C_F\ H\ N \tag{12}$$

where H is the mean height of ridges, N is the number of ridges per unit downwind distance, C_{10} is a flat-plate drag coefficient describing the drag due to undeformed ice and C_F is a form drag coefficient. Bank et al. found that C_{10} varies only over a limited range (1.3 to 2.1 x 10^{-3}). C_F is a function of the slope angle of ridges, and for a large aggregation of ridges is probably a constant, in the range 0.3 to 0.4. Therefore the variation in overall drag is largely governed by the variation in the numbers and mean heights of ridges. This is important in modelling both the MIZ and the shear zone, since we have seen in section 3 how the shear zone is characterized by intense ridging. In the marginal ice zone an additional factor comes into play in the form of the vertical edges of floes, which make their own contribution to the form drag. Thus although the marginal ice zone has a lesser degree of ridging than the central Arctic (and certainly far less than the shear zone) it is by no means certain that the overall drag coefficients are less. Laser and sonar profiles across the marginal zone are required to determine this question.

Of available profiles, the most relevant are those of Kozo and Tucker (1974) obtained by submarine in winter (March) across the Denmark Strait between 67° and 70°N. A variety of analyses was performed on the data. Spectral analysis showed that the ice bottom profile approximated to a red noise spectrum. The standard deviation increased with distance from the ice edge, and the number of Fourier components required to account for most of the variance decreased (in other words, long wavelength roughness began to predominate over short wavelength roughness). They identified four regimes of ice, moving inwards from the ice edge, followed by a fifth regime identical to central Arctic ice; thus they were able to identify the width of the marginal ice zone which they found to be 165 km. It is worthwile describing their regimes in detail:

Regime 1. 0-58 km. Floes ranged from pancake ice 3 m across to small floes less than 50 m across. No measurable ridges. Standard deviation 1 m.

Regime 2. 58-94 km. Floe diameters 50-75 m. Shallow ridges less than 5 m deep appear. Standard deviation still only 1.2 m.

Regime 3.108-153 km. A transition zone. Long wavelength variance still low, s.d. still only 1.5 m, but ridge drafts and frequencies increasing, causing greater drag and floe motion. Floe diameters still 50-100 m.

Regime 4.153-166km. End of marginal ice zone. The leading edges of low-pressure cells in the Denmark Strait push individual ice floes towards the Greenland coast, the result being compaction and deformation. Floe diameters 100-150 m. Keel frequencies increasing, and drafts to 12 m. s.d. rises to 2 m, and long wavelength variance increases. Floes increase to 150 m diameter, but with wider size variations.

Regime 5. 166 km on. Identical to central Arctic ice with respect to ridge frequencies and draft. Multiyear floes begin, some over 400 m across, causing increasing long wavelength variance and an s.d. increasing to 3-4 m.

Although this is only a single section across a particular MIZ the characteristics are very typical of MIZ's in general. We conclude that the restricted keel drafts in regimes 1-4 probably overcome the effect of floe edges so that the drag coefficient increases smoothly with penetration until it reaches its normal central Arctic value. A modeller might therefore take some smooth function which will tail off his central Arctic drag coefficient C to zero at the ice edge. A possible function would be

$$C_s = C\,[1 - \exp(-\lambda s)] \qquad (13)$$

where s is distance from ice edge in km and λ is about 70-100 km^{-1}.

These results refer to under-ice roughness, but the experiments reported by Kozo and Tucker also included laser profiles over the same area. Kozo and Diachok (1973) reported on a joint analysis of the laser and sonar profiles, and Figure 14 shows their results for the frequencies of keels and sails as a function of distance from the ice edge. It can be seen that the frequencies reach a peak some 170 km inside the ice edge, roughly corresponding with the shelf break (where the core of maximum current velocity occurs). The distribution of sail heights and keel drafts also changed radically with distance from the ice edge (Figure 15), with the bigger elevations becoming more common at increasing penetration. The normalized distributions of sail and keel elevations appeared to be superposable if the keel draft was taken as five times the sail height. It is clear from Figures 14 and 15 that the topside drag coefficient falls off as the ice edge is approached in the same way as the bottomside coefficient. Kozo and Diachok estimated that 'the region of easy penetration of swell and waves' extended 90 km

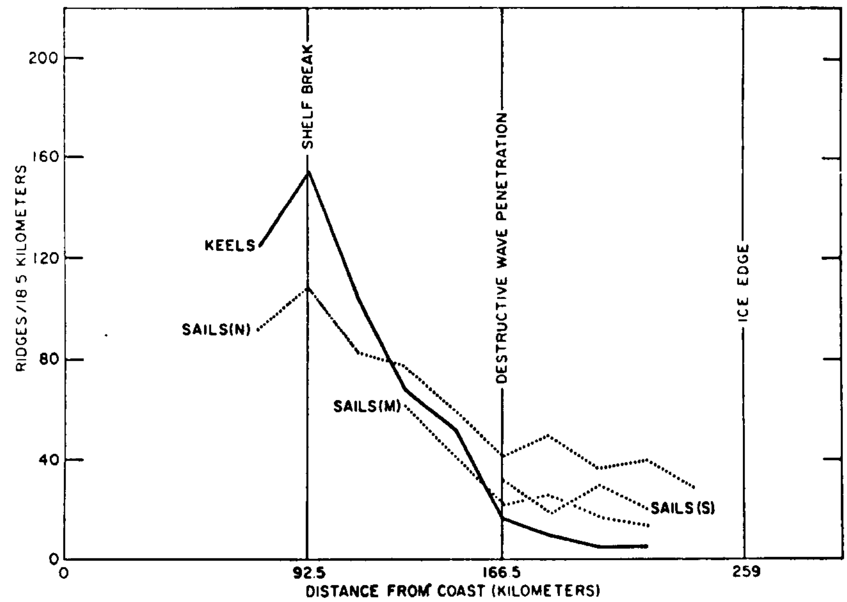

Figure 14. Frequencies of keels and sails from transects across Denmark Strait (after Kozo an Diachock, 1973).

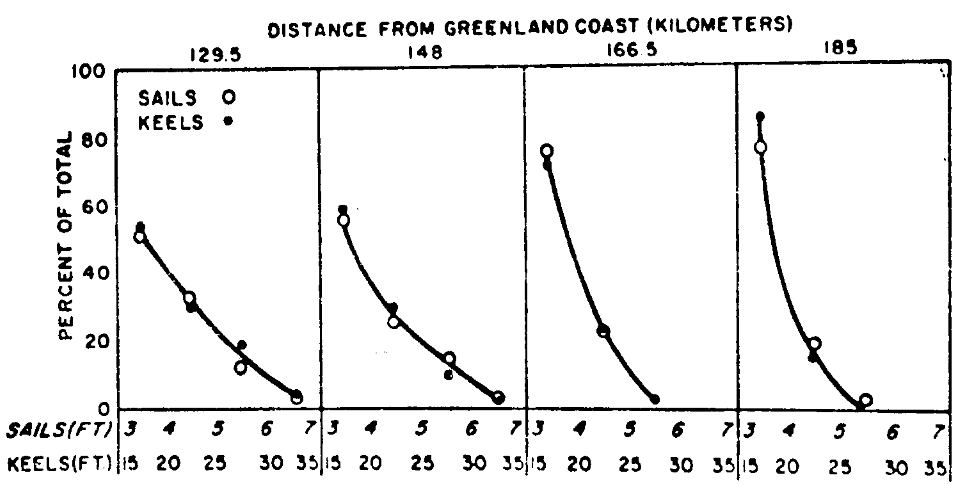

Figure 15. Normalized distributions of keel drafts and sail elevations (after Kozo and Diachok, 1973).

from the ice edge. At the time of the experiment their laser profilometer recorded a 7 s wave which had an amplitude of 15 cm in the thin edge ice and which was detectable for 45 km inside the ice edge. The ice edge region had a very diffuse ice cover with only 10-20% ice, so that

45 km penetration is equivalent to only 4.5-9 km through a compact ice cover, and this is in fact the skin depth for 7 s waves found by Wadhams (1975, 1978b).

A third report on the results of the same flights was made by Ketchum and Wittmann (1972), concentrating on infra red line scan and photographic imagery of the marginal pack, and its relationship to meteorological forcing. The IR imagery presented in this paper depicts in the clearest possible way the "extreme wreckage" of ice resulting from the wave and wind action and is perhaps the best imagery yet obtained of the quintessential MIZ.

Young ice forms found in MIZ

When new ice forms in the central Arctic in a freshly opened lead, it proceeds rapidly from an initial skim of independent crystals to a coherent sheet. The only exceptions are if a strong wind is blowing, or if there is a powerful surface current in the lead which may sweep the new crystals under the neighboring floe edge. In the MIZ the whole ice pack is exposed to swell action, and the fragmented nature of the ice results in large connected areas of open water which allow the wind sufficient fetch to generate a significant local chop. Under these circumstances the new ice grows into a thick soup of independent crystals (frazil or grease ice) before partially metamorphising into small plates 1-2 m across and some 30 cm thick with raised rims (pancake ice). Only later are these cakes cemented together to form a coherent ice sheet. Figs. 15a and 15b show two stages in this process. As Scoresby (1820) wrote:

> "Whenever ice does occur in agitated waters, its exterior is always sludge, and its interior pancake ice, the pieces of which gradually increase in size with the distance from the edge".

The physical properties of frazil and pancake ice have been investigated by Martin (1979) and Martin et al. (1978) in field and laboratory studies. The transition from frazil to pancake was found to occur quite suddenly after the frazil suspension reached a critical depth and crystal density, and the size of the subsequent pancakes was related to the wavelength of the local wave field. The raised rims around the pancakes are formed by pumping action; as the waves force the pancakes together water is pumped up over the cake edges and freezes on top of the cake. The ice sheet that later forms from the pancakes has a very high surface salinity. Martin mentions a third form of young ice, which is created when blowing snow accompanies the local wind; under these circumstances the snow and frazil mix to create a type of slush ice.

The importance of frazil ice lies in the fact that its thermal conductivity is almost as high as open water, so that a layer of frazil ice 30 cm thick, containing say 40% ice in the suspension, has a far higher heat flow through it than an ice sheet 12 cm thick, although the mass of ice is the same.

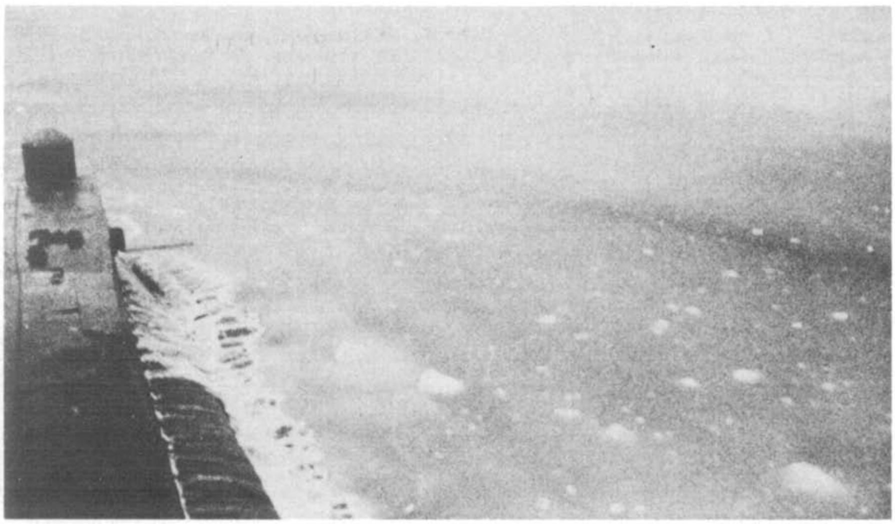

Figure 15a. Grease ice with lumps of shuga. Greenland Sea, February.

Figure 15b. Pancake ice. Greenland Sea, February.

Problems of Modelling the MIZ

Prospective modellers of the MIZ are likely to have one of four aims in view:

(i) to develop a regional model of a whole drift system, e.g., the East Greenland or Labrador Current;

(ii) to predict small scale motions of the ice edge for the immediate use of clients such as oil drilling ships, cargo or fishing vessels;

(iii) to predict mesoscale motions of the ice margin, e.g., seasonal or annual changes in ice limits, for the benefit of countries such as Iceland that will be affected thereby;

(iv) to predict the large scale seasonal advance and retreat of the ice cover for coupling with atmospheric models of the whole hemisphere.

(ii) can be accomplished by elaborations of well-known rules of thumb such as Zubov's law. (iv) is once again the domain of ocean-wide modelling, and it is unlikely that the modified properties of the MIZ will have a large effect on these gross ice limits. As it is, models which are specifically designed to be coupled to atmosphere models (e.g., Parkinson and Washington, 1979) are greatly over-simplified and yet predict the advance and retreat reasonably well. The properties of the MIZ are therefore likely to be most important in models of types (i) and (iii).

The properties of the MIZ which a modeller may have to take into account are as follows:

1. The nature of the ice cover. The breakup into floes with a floe size that becomes smaller as the ice edge is approached means that the open water component cannot just be modelled as a compactness term, but instead must be modelled in terms of average floe size, on account of lateral melting which depends on floe perimeter.

2. The presence of a front. Under this heading we include a large number of oceanographic factors which occur at the ice margin due to the nearness of warm surface water. In particular, eddies in the front transport heat into the ice zone and ice out of it, while any ice which is driven across the Front by the wind is lost to the ice zone.

3. Heat fluxes. There is lateral melting around floes and wave-induced melting under them to add to the heat balance in summer. The upper mixed layer is affected to an unknown extent by the input of salt from winter freezing and the input of melt water in summer, both of which occur at a greater rate than in the central Arctic. The large areas between floes induce rapid ice growth and salt rejection in winter, which may have a strong effect on the mixed layer and thus on the ocean-atmosphere heat flow.

4. Internal stresses and ice drift. Internal stresses are quite different from those in the central Arctic, and are probably transmitted over a shorter range by means of collisions rather than continuous forces. Thus ridge-building, if any, occurs in a quite different way and so the ice thickness redistribution term in ice models has to be changed as well. An icefield which drifts almost freely is subject to inertial oscillations (Hunkins, 1967). Neglecting these, McPhee (1979) considered how a free-drift model could account for ice motion at the AIDJEX sites in summer. He considered the force balance on a unit area of continuous ice sheet, neglecting the internal stress term. A modified version of his balance, applicable to an isolated floe, is shown in Figure 16. Here $\underline{V}$ is the steady state ice drift relative to the undisturbed ocean surface current, m, a, h, are the mass, area and thickness of the floe and f is the Conolis parameter. The wind force term, which uses the wind velocity $\underline{U}_{10}$ at anemometer height, has a drag coefficient C which is given by (12) and which must include an important form drag component, since for a small floe the leading edge and any surface protuberances may yield drags far greater than the flat surface. The form drag will be a function of (h/a). The

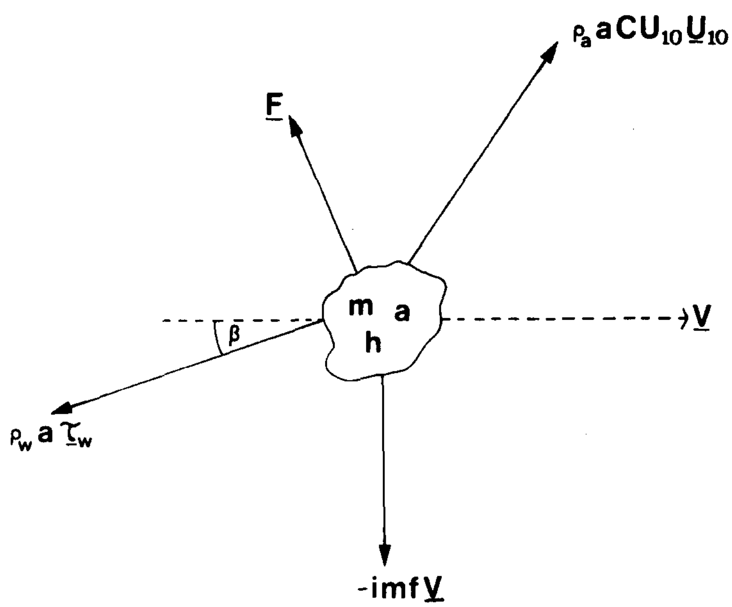

Figure 16. Force balance on an isolated floe.

term F is the wave radiation force, given by (10). The water drag term includes the stress term $\underline{\tau}_w$ which is given in the AIDJEX model (McPhee, 1975) by

$$\underline{\tau}_w = -c_w V \underline{V} e^{i\beta} \tag{14}$$

where c_w and β are experimentally determined boundary layer values. In the case of an isolated floe c_w must include an addition for form drag, again a function of (h/a) and likely to be important if not dominant; and β may well be small since an ice-water boundary layer cannot develop fully under a small floe. Therefore even steady-state drift is difficult to model, and such an apparently simple problem as deriving the relative drift speeds of floes of different sizes in the same wind is impossible to solve accurately. Much more experimental data is necessary on floe drift speeds in the MIZ.

Problems of modelling are discussed further in Solomon (1972), Rothrock (1978) and Doronin and Kheisin (1977, ch. 12); the latter authors deal with the techniques adopted in the Soviet Union, which have considerable success in predicting, for instance, the ice limits in the Kara Sea. They point out that models of type (ii), i.e., site-specific small scale models, are made more complicated for coastal areas by the presence of tidal currents; the semidiurnal tidal frequency and the inertial frequency are almost identical at high latitudes.

ANTARCTIC SEA ICE

Our review of Antarctic sea ice will be brief, not because there are few problems but because there are few facts. The first fact is that nearly all of the Antarctic is a seasonal ice zone. It has been estimated (Treshnikov, 1966) that the yearly variation in the area of the ice cover is 75% of the maximum, compared with only 25% for the Arctic. The main areas in which pack ice remains during the summer are the Weddell Sea and parts of the Ross and Bellingshausen Seas (Atlas Antarktiki, 1966; Mackintosh, 1972), and so it is only in these areas that significant amounts of multi-year ice can be found. The vast perimeter of the Antarctic winter ice cover means that a large proportion of the Antarctic ice can be considered as MIZ - in fact, with the enomous fetch and strong winds of the Southern Ocean and the velocity shear across the Antarctic Polar Front this is really the classic case of an MIZ. Thus a large part of the Antarctic is subject to the phenomena described in section 4, with all the implications that this involves for modelling. Modelling of the Antarctic ice cover is only in its early stages (Kulakov et al., 1979; Parkinson and Washington, 1979) yet is of great climatic importance since during the southern winter the Antarctic sea ice covers a greater area than the Arctic ice does during the northern winter (Fletcher, 1969).

Studies of the climatic effects of Arctic ice have been greatly assisted by the data provided by the electronically scanning microwave radiometer (ESMR) aboard the Nimbus V statellite (Zwally and Gloersen, 1977). Not only does this provide data on the overall extent of the ice cover, but it also gives a measure of the percentage ice cover within the ice margin. Using this data Budd (1975) and Ackley and Keliher (1976) investigated ice-climate interactions. Their first general conclusion, already well known, is that the Antarctic ice cover is everywhere divergent in its mean behavior, moving northward under the prevailing wind field and thus constantly opening new leads and polynyas. This divergence also affects the response of the ice to atmospheric lows. In winter a concentrated ice pack acts as viscous material and responds to a low by converging. However, if the ice is divergent and loose it responds to a low by diverging further, allowing greater heat loss to the atmosphere which strengthens the low still more, providing a positive feedback mechanism to exacerbate atmospheric fluctuations.

Another result of the net divergence of the Antarctic ice is the existence of a chain of semi-permanent polynyas around the coast of the continent through the winter (Knapp, 1972). These are kept open by katabatic winds and Southern Ocean cyclones which sweep away the sea ice as fast as it forms.

Antarctic sea ice differs in many respects from Arctic ice; Buynitskiy (1967) and Lewis and Weeks (1971) have reviewed studies made up to 1970. The structure of the ice usually includes a layer of "infiltration ice" near the surface, formed either from the flooding of the ice surface as it sinks under the weight of a snow cover, or else from an initial growth from the slushy snow-frazil mixture reported by Martin (1979). Such a layer is uncommon in Arctic ice because precipitation is much lower in the Arctic so that an ice cover seldom acquires enough snow to make it sink below sea level. Two other features once thought peculiar to Antarctic ice have also been observed in the Arctic. One is "underwater ice" or "anchor ice" which is scattered in plates through the normal columnar structure of the lower part of the ice sheet. This is believed to form in the water column just under the ice sheet and to float up against the growing ice-water interface, and it is a feature of ice growing by convection in shallow water. It has been observed in McMurdo Sound and is common along the Bering Sea coast of Alaska. An associated phenomenon is that of ice stalactites, long features enclosing the exit tubes of brine drainage channels. These were first discovered in McMurdo Sound (Daytin and Martin, 1971) and a theory of their formation was given by Martin (1974). They too have been observed in the Arctic (Lewis and Milne, 1977).

Finally, the geometry of Antarctic ice is scarcely known at all. It is known that first-year ice, when undeformed, grows to a greater thickness in the Antarctic (2.75-3.35 m. Paige, 1966) than in the Arctic (2.0-2.2 m, Thorndike et al., 1975). However, since Antarctic ice is almost all first-year, the overall mean ice thickness is probably lower in the Antarctic than in the Arctic. Furthermore, observers report little ridging in the Antarctic, whereas in the Arctic a considerable fraction of the total ice mass (perhaps as much as 40%) is contained in deformation structures such as pressure ridges. It is astonishing to realize that not a single airborne laser profile or submarine sonar profile has been obtained from the Antarctic to give some quantitative estimate of the degree of roughness of the ice cover. Such a profile would provide information on ridging extents, the nature of deformation structures (if any), and the values of surface and bottom drag coefficients that would be appropriate for the modelling of Antarctic ice drift.

REFERENCES

Ackley, S.F. and T.E. KELIHER (1976), Antarctic sea ice dynamics and its possible climatic effects. AIDJEX Bull., 33:54-76.

Alekseev, G.V. and A. Yu. BUZUEV (1973), Bokovoe tayanie l'da v razvod'yakh (Lateral melting of ice in leads). Trudy AANII, 307:169-178

Allan, A.J., P. Wadhams and A.M. Cowan (1979), An experimental study of wave-ice interaction and floe flexure in the pack ice of the Labrador Current. Centre for Cold Oceans Resources Engng., Memorial Univ., St. John's, Tech. Rept., in press.

Anderson, D.L. (1963), Use of long-period surface waves for determination of elastic and petrological properties of ice masses. In Ice and Snow, (W.D. Kingery, ed.), M.I.T. Press, Cambridge, Mass., 63-68.

Assur, A. (1963), Breakup of pack-ice floes. In Ice and Snow, (W.D. Kingery, ed.), M.I.T. Press, Cambridge, Mass., 335-347.

Atlas Antarktiki (1966), Gidrometeoizdat, Leningrad.

Banke, E.G., S.D. Smith and R.J. Anderson (1976), Recent measurements of wind stress on Arctic sea ice. J. Fish. Res. Bd. Canada, 33(10):2307-2317.

Bilello, M.A. (1979), Decay patterns of landfast sea ice in Canada and Alaska. In Sea Ice Processes and Models, (R.S. Pritchard, ed.), Univ. Washington Press, Seattle, in press.

Budd, W.F. (1975). Antarctic sea-ice variation from satellite sensing in relation to climate. J. Glaciol., 15(73):417-428

Buynitskiy, V.Kh. (1967), Structure, principal properties and strength of Antarctic sea ice. Soviet Antarctic Exped. Information Bull, 65:90-104. (Eng. Trans. 6(6):504).

Campbell, W.J. and A.S. Orange (1974), The electrical anisotropy of sea ice in the horizontal plane. J. Geophys. Res., 79(33):5059-5063.

Campbell, W.J., W.F. Weeks, R.O. Ramseier and P. Gloersen (1975), Geophysical studies of floating ice by remote sensing. J. Glaciol., 15(73):305-328.

Cherepanov, N.V. (1964), Struktura morskikh l'dov bol'shoi tolschiny (Structure of very thick sea ice. Trudy AANII, 267:13-18.

Cherepanov, N.V. (1971), Prostranstvennaya uporyadochennost' Kristallicheskoi morskikh l'dov (Spatial arrangement of sea ice crystal structure). Problemy Arktiki i Antarktiki, 38:137-140.

Coachman, L.K. and C.A. BARNES (1961), The contribution of Bering Sea water to the Arctic Ocean. Arctic, 14(3):146-161.

Cooper, P.F. (1974), Landfast ice in the southeastern part of the Beaufort Sea. In The Coast and Shelf of the Beaufort Sea, (J.C. Reed, J.F. Sater, eds.), Arctic Inst. N. Amer., Arlington, 235-242.

Cox, G.F.N. and W.F. Weeks (1974), Salinity variations in sea ice. J. Glaciol., 13(67), 109-120.

Csanady, G.T. (1972), Geostrophic drag, heat and mass coefficients for the diabatic Ekman layer. J. Atmos. Sci., 29:488-496.

Dayton, P.K. and S. Martin (1971), Observations of ice stalactites in McMurdo Sound, Antarctica. J. Geophys. Res., 76(6):1595-9.

Dean, C.H. (1966), The attenuation of ocean waves near the open ocean/pack ice boundary Symp. on Antarctic Oceanogr., Scott Polar Res. Inst., Cambridge, 221-222 (Abstr.)

Diachok, O.I. and R.S. Winokur (1974), Spatial variability of underwater ambient noise at the Arctic Ice-water boundary. J. Acoust. Soc. Am., 55(4).

Doronin, Yu.P. and D.E. Kheisin (1977), Sea Ice. Leningrad, Gidrometeoizdat, 1975. Eng. Trans. 1977 by Amerind Publishing Co. Pvt. Ltd., New Delhi. 323 pp.

Einarsson, T. (1972), Sea currents, ice drift, and ice composition in the East Greenland Current. In Sea Ice (t. Karlsson ed.), Nat. Res. Counc. of Iceland, Reykjavik, 23-32.

Fletcher, J.O. (1969), Ice extent in the Southern Ocean and its relation to world climate. Rand Corpn., Santa Monica, Rept. RM-S793-NSF.

Francois, R.E. and W.K. Nodland (1972). Unmanned Arctic Research Submersible (UARS) system development and test report. Applied Phys. Lab., Univ. Washington, Seattle, Tech. Rept. APL-UW 7219, 88 pp.

Goodman, D.J. (1977), Creep and friction of ice and surface strain measurements on glaciers and sea ice. Ph.D. Thesis, Univ. of Cambridge, Dept. Physics.

Goodman, D.J., A.J. Allan and R.G. Bilham (1975), Wire strainmeters on ice. Nature, Lond., 255:45-46.

Goodman, D.J. and D. Tabor (1978), Fracture toughness of ice: a preliminary account of some new experiments. J. Glaciol., 21(85):651-660.

Greenhill, A.G. (1887), Wave motion in hydrodynamics. Amer. J. Math., 9:62-212.

Hibler, W.D. III (1978), Model simulations of near shore ice drift, deformation and thickness. Proc. 4th Intl. Conf. Port and Ocean Engng. Under Arctic Condns. (D.B. Muggeridge, ed.), Memorial Univ., St. John's, 1:33-44.

Hibler, W.D. III (1979), A dynamic thermodynamic sea ice model. J. Phys. Oceanogr., in press.

Hibler, W.D. III, S.F. Ackley, W.K. Crowder, H.L. McKim and D.M. Anderson (1974), Analysis of shear zone ice deformation in the Beaufort Sea using satellite imagery. In The Coast and Shelf of the Beaufort Sea, (J.C. Reed, J.F. Sater, eds.), Arctic Inst. N. Amer., Arlington, 285-296.

Hunkins, K. (1962), Waves on the Arctic Ocean. J. Geophys. Res., 67(6):24772489.

Hunkins, K. (1967), Inertial oscillations of Fletcher's ice island (T3). J. Geophys. Res., 782:1165-1174.

Johannessen, O.M. and L.A. Foster (1978), A note on the topographically controlled oceanic polar front in the Barents Sea. J. Geophys. Res., 83(C9):4567-4571.

Jones, S. (1977), Instabilities and wave interactions in a rotating two-layer fluid. Ph.D. thesis, Univ. Cambridge.

Keliher, T.E. (1967), An investigtion of the effect of large-amplitude ocean waves on Antarctic pack ice. AIDJEX Bull., 34:114-136.

Ketchum, R.D. and W.I. Wittmann (1972), Recent remote sensing studies of the East Greenland pack ice. In Sea Ice (T. Karlsson, ed.), Nat. Res. Counc. Iceland, Reykjavik, 213-226.

Knapp, W.W. (1972), Satellite observations of large ploynyas in Polar waters. In Sea Ice (T. Karlsson, ed.), Nat. Res. Counc. Iceland, Reykjavik, 201-212.

Kovacs, A. and M. Mellor (1974), Sea ice morphology and ice as a geological agent in the southern Beaufort Sea. In The Coast and Shelf of the Beaufort Sea, (J.C. REED, J.E. Sater, eds.), Arctic Inst. N. Amer., Arlington, 113-161.

Kovacs, A. and R.M. Morey (1978), Radar anisotropy of sea ice due to preferred azimuthal orientation of the horizontal c axes of ice crystals. J. Geophys. Res., 83(C12):6037-6046.

Kozo, T.L. and O.I. Diachok (1973), Spatial variability of topside and bottomside ice roughness and its relevance to underside acoustic reflection loss. AIDJEX Bull., 19:113-121.

Kozo, T.L. and W.B. Tucker (1974), Sea ice bottomside features in the Denmark Strait. J. Geophys. Res., 79(30):4505-4511.

Kulakov, I.Yu., M.I. Maslovsky and L.A. Timokhov (1979), Seasonal variability of Antarctic sea ice extent: its numerical modelling. In Sea Ice Processes and Models (R.S. Pritchard, Ed.), Univ. Washington Press, Seattle, in press.

Leblond, P.H. and L.A. Mysak (1978), Waves in the Ocean. Elsevier, Amsterdam, 602pp.

Legeckis, R. (1978), A survey of worldwide sea surface temperature fronts detected by environmental satellites. J. Geophys. Res., 83(C9):45014522.

Lewis, C.F.M. (1975), Bottom scour by sea ice in the southern Beaufort Sea. Beaufort Sea Proj. Tech. Rept. 23, Queen's Printer, Ottawa.

Lewis, E.L. and A.R. MILNE (1977), Underwater sea ice formations. In Polar Oceans (M.J. Dunbar, ed.), Arctic Inst. N. Amer., Calgary, 239-245.

Lewis, E.L. and W.F. Weeks (1971), Sea ice: some polar contrasts. In Symp. on Antarctic Ice & Water Masses, Sci. Comm. Antarctic Res., Cambridge, 23-34.

Lindsay, D.G. (1969), Ice distribution in the Queen Elizabeth Islands. In Ice Seminar, Special Vol. 10, Can. Inst. Min. Metall., 45-60.

Longuet-Higgins, M.S. (1977), The mean forces exerted by waves on floating or submerged bodies with applications to sand bars and wave power machines. Proc. R. Soc. Lond., A, 352:463-480.

Lyon, W. (1967), Under surface profiles of sea ice observed by submarine. In Physics of Snow and Ice, Hokkaido Univ., Sapporo, 1(1):707-711.

Mackintosh, N.A. (1972), Life cycle of Antarctic krill in relation to ice and water conditions. Discovery Reports, 36, 1-94.

McPhee, M.G. (1975), Ice-ocean momentum transfer for the AIDJEX model. AIDJEX Bull., 29:93-111.

McPhee, M.G., (1979), An analysis of pack ice drift in summer. In Sea Ice Processes and Models (R.S. Pritchard, ed.), Univ. Washington Press, Seattle, in press.

Marko, J.R. and R.E. Thomson (1975), Spatially periodic lead patterns in the Canada Basin sea ice: a possible relationship to planetary waves. Geophys. Res. Letters, 2(10): 431-434.

Marko, J.R. and R.E. Thomson (1976), Rectilinear leads and internal motions in the ice pack of the western Arctic Ocean. J. Geophys. Res., 82(6): 979-987.

Martin, S. (1974), Ice stalactites: comparison of a laminar flow theory with experiment. J. Fluid Mech., 63,:51-79.

Martin, S. (1979), A field study of brine drainage and oil entrapment in first year sea ice. J. Glaciol., in press.

Martin, S., P. Kauffman and P.E. Welander (1978), A laboratory study of the dispersion of crude oil within sea ice grown in a wave field. Proc. 27th Alaska Science Conf., (G.C. West, ed.), Amer. Assoc. Advancement of Sci., Fairbanks, in press.

Mills, D.A. (1972), On waves in a sea ice cover. Res. paper 53, Horace Lamb Centre for Oceanogr. Res., Flinders Univ. of S. Australia, Bedford park. 64pp.

Milne, A.R. (1972), Thermal tension cracking in sea ice: a source of underice noise. J. Geophys. Res., 77(12):2177-2192.

Mock, S.J., A.D. Hartwell and W.D. Hibler III (1972), Spatial aspects of pressure ridge statistics. J. Geophys. Res., 77(30):5945-5953.

Muench, R.D. and R.L. Charnell (1977), Observations of medium-scale features along the seasonal ice edge in the Bering Sea. J. Phys. Oceanogr., 7(4):602-606.

Neal, V.T. and W.D. Nowlin (1979), International Southern Ocean Studies of circumpolar dynamics. Polar Record, 19(122), in press.

Paige, R.A. (1966), Crystallographic studies of sea ice in McMurdo Sound, Antarctica. U.S. Nav. Civ. Engng. Lab., Tech. Rept. R494, 1-31.

Parkinson, C.L. and W.M. Washington (1979), Summary of a large-scale sea ice model. In Sea Ice Processes and Models (R.S. Pritchard, ed.), Univ. Washington Press, Seattle, in press.

Parmerter, R.R. (1975), On the fracture of ice sheets with part-through cracks. AIDJEX Bull., 30:94-118.

Pelletier, B.R. and J.M. Shearer (1972), Sea bottom scouring in the Beaufort Sea of the Arctic Ocean. In Marine Geology and Geophysics, Proc. 24th Intl. Geol. Congress, Sec. 8, 251-261.

Pounder, E.R. (1965), The Physics of Ice. Pergamon, Oxford. 151pp.

Pritchard, R.S. (1979), A simulation of nearshore winter ice dynamics in the Beaufort Sea. In Sea Ice Processes and Models (R.S. Pritchard, ed.), Univ. Washington Press, Seattle, in press.

Pritchard, R.S., M.D. Coon, M.G. McPhee and E. Leavitt (1977), Winter Ice dynamics in the nearshore Beaufort Sea. AIDJEX Bull., 37:37-94.

Reimnitz, E. and P.W. Barnes (1974), Sea ice as a geologic agent on the Beaufort Sea shelf of Alaska. In The Coast and Shelf of the Beaufort Sea, (J.C. Reed, J.E. Sater, eds.), Arctic Inst. N. Amer., Arlington, 301-353.

Reimnitz, E., L. Toimil and P. Barnes (1977), Arctic continental shelf processes and morphology related to sea ice zonation, Beaufort Sea, Alaska. AIDJEX Bull., 36:15-64.

Robin, G. de Q. (1963), Wave propagation through fields of pack ice. Phil Trans. R. Soc. Lond., A 255(1057):313-339.

Rothrock, D.A. (1978), Modelling sea ice features and processes. Presented at Symp. on Dynamics of Large Ice Masses, Ottawa, Aug. 1978.

Scoresby, W. (1820), An Acccount of the Arctic Regions, with a History and Description of the Northern Whale-Fishery. 2 vols. Constable, Edinburgh. Reprinted 1969, David and Charles Reprints, Newton Abbot.

Shearer, J.M. and S. Blasco (1975), Further observations of the scouring phenomena in the Beaufort Sea. Geol. Survey Canada, Ottawa, Paper 75-1, A, 483-493.

Sodhi, D.S. (1977), Ice arching and the drift of pack ice through restricted channels. U.S. Army CRREL Rept. 77-18, 11pp.

Sodhi, D.S. and W.D. Hibler III (1979), A finite element formulation of a sea ice drift model. In Sea Ice Processes and Models, (R.S. Pritchard, ed.), Univ. Washington Press, Seattle, in press.

Solomon, H. (1970), A study of ice dynamics relevant to AIDJEX. AIDJEX Bull. 2:33-50.

Solomon, H. (1972), Note on the no-stress boundary condition at the edge of the ice pack. Arctic, 25(1):57-8.

Squire, V.A. (1979), Dynamics of ocean waves in a continuous sea ice cover. Ph.D. Thesis, Univ. of Cambridge, 191pp.

Squire, V.A. and A.J. Allan (1979), Propagation of flexural gravity waves in sea ice. In Sea Ice Processes and Models, (R.S. Pritchard, ed.), Univ. Washington Press, Seattle, in press.

Stringer, W.J. (1974), Sea ice morphology of the Beaufort shorefast ice. In The Coast and Shelf of the Beaufort Sea (J.C. Reed, J.E. Sater, eds.), Arctic Inst. N. Amer., Arlington, 165-172.

Thorndike, A.S., D.A. Rothrock, G.A. Maykut and R. Colony (1975), The thickness distribution of sea ice. J. Geophys.Res., 80:4501-4513.

Treshnikov, A.F. (1966), The ice of the Southern Ocean. Proc. Symp. on Pacific-Antarctic Sci., Japanese Antarctic Res. Expdn. Sci. Repts., Special Issue no. 1.

Tucker, W.B., W.F. Weeks, A. Kovacs and A.J. Gow (1979a), Nearshore ice motion at Prudhoe Bay, Alaska. In Sea Ice Processes and Models, R.S. Pritchard, ed.), Univ. Washington Press, Seattle, in press.

Tucker, W.B., W.F. Weeks and M. Frank (1979b), Sea ice ridging over the Alaskan continental shelf. J. Geophys. Res., in press.

Verrall, R.I., J.H. Ganton and A.R. Milne (1974), An ice drift measurement in western Parry Channel. Arctic, 27(1):47-52.

Vinje, T.E. (1977), Sea ice studies in the Spitzbergen-Greenland area. Landsat Rept. E77-10206, US Dept. of Commerce, Natl. Tech. Info. Service, Springfield, Va.

Wadhams, P. (1972), Measurement of wave attenuation in pack ice by inverted echo sounding. In Sea Ice (T. Karlsson, ed.), Natl. Res. Counc. of Iceland, Reykjavik, 255-260.

Wadhams, P. (1973a), Attenuation of swell by sea ice. J. Geophys. Res., 78(18):3552-3563.

Wadhams, P. (1973b), The effect of a sea ice cover on ocean surface waves. Ph.D. thesis, Univ. Cambridge. 223pp.

Wadhams, P. (1975), Airborne laser profiling of swell in an open ice field. J. Geophys. Res., 80:4520-4528.

Wadhams, P. (1976), Sea ice topography in the Beaufort Sea and its effect on oil containment. AIDJEX Bull., 33:1-52.

Wadhams, P. (1978a), Characteristics of deep pressure ridges in the Arctic Ocean. Proc. 4th Intl. Conf. Port & Ocean Engng. Under Arctic Condns.,(D.B. Muggeridge, ed.), Memorial Univ., St. John's, 1, 544-555.

Wadhams, P. (1978b), Wave decay in the marginal ice zone measured from a submarine. Deep-sea Res., 25:23-40.

Wadhams, P. (1979), A comparison of sonar and laser profiles along corresponding tracks in the Arctic Ocean. In Sea Ice Processes and Models (R.S. Pritchard, ed.), Univ. Washington Press, Seattle, in press.

Wadhams, P. (1979b), Field experiments on wave-ice interaction in the Labrador and East Greenland Currents, 1978. Polar Record, 19(121):373-376.

Wadhams, P. (Unpubl.), A further analysis of sonar and laser profiles from corresponding tracks in the Arctic Ocean. To be submitted to J. Glaciol.

Wadhams, P., A.E. Gill and P.F. Linden (1979), Transects by submarine of the East Greenland Polar Front. Deep-Sea Res., in press.

Wadhams, P. and R.J. Horne (1978), An analysis of ice profiles obtained by submarine sonar in the AIDJEX area of the Beaufort Sea. Scott Polar Res. Inst., Cambridge, Tech. Rept. 78-1, 65pp.

Wadhams, P. and R.T. Lowry (1977), A joint topside-bottomside remote sensing experiment on the Arctic sea ice. Proc. 4th Can. Symp. on Remote Sensing, Can. Remote Sensing Soc., Ottawa, 407-423.

Walker, E.R. and P. Wadhams (1979), On thick sea-ice floes. Arctic, in press.

Weber, J.R. and M. Erdelyi (1976), Ice and ocean tilt measurements in the Beaufort Sea. J. Glaciol., 17(75):61-71.

Weeks, W.F. (1976), Sea ice properties and geometry. AIDJEX Bull., 34:137-172.

Weeks, W.F. and A. Assur (1967), The mechanical properties of sea ice. Rept. II-C3, U.S. Army CRREL, Hanover. 80pp.

Weeks, W.F. and A.J. Gow (1978), Preferred crystal orientations in the fast ice along the margins of the Arctic Ocean., Rept. 78-13, U.S. Army CRREL, Hanover. 24pp.

Weeks, W.F., A. Kovacs and W.D. Hibler III (1971), Pressure ridge characteristics in the Arctic coastal environment. Proc. 1st Intl. Conf. Port and Ocean Engng. Under Arctic Conditions., Tech. Univ., Trondheim, 1:152-182.

Weeks, W.F., W.B. Tucker, M. Frank and S. Fungcharoen (1979), Characterization of the surface roughness and floe geometry of the sea ice over the continental shelves of the Beaufort and Chukchi Seas. In Sea Ice Processes and Models, (R.S. Pritchard, ed.), Univ. Washington Press, Seattle, in press.

Wetzel, V.F., R.K. Atwater and T.E. Huta (1974), Arctic ice movement and environmental data stations. In The Coast and Shelf of the Beaufort Sea, (J.C. Reed, J.E. Sater, eds.), Arctic Inst. N. Amer., Arlington, 269-284.

Zubov, N.N. (1945), Arctic Ice. Izdatel'stvo Glavsermorputi, Moscow. Eng. trans. U.S. Navy Oceanogr. Off./Amer. Met. Soc.

Zwally, H.J. and P. Gloersen (1977), Passive microwave images of the polar regions and research applications. Polar Record, 18(116):431-450.